Topics in Current Chemistry (2020) 378:40
https://doi.org/10.1007/s41061-020-00302-w

REVIEW

Magnetic Nanoparticles as MRI Contrast Agents

Ashish Avasthi[1] · Carlos Caro[1] · Esther Pozo-Torres[2] · Manuel Pernia Leal[2] · María Luisa García-Martín[1,3]

Received: 31 December 2019 / Accepted: 18 March 2020

Abstract

Iron oxide nanoparticles (IONPs) have emerged as a promising alternative to conventional contrast agents (CAs) for magnetic resonance imaging (MRI). They have been extensively investigated as CAs due to their high biocompatibility and excellent magnetic properties. Furthermore, the ease of functionalization of their surfaces with different types of ligands (antibodies, peptides, sugars, etc.) opens up the possibility of carrying out molecular MRI. Thus, IONPs functionalized with epithelial growth factor receptor antibodies, short peptides, like RGD, or aptamers, among others, have been proposed for the diagnosis of various types of cancer, including breast, stomach, colon, kidney, liver or brain cancer. In addition to cancer diagnosis, different types of IONPs have been developed for other applications, such as the detection of brain inflammation or the early diagnosis of thrombosis. This review addresses key aspects in the development of IONPs for MRI applications, namely, synthesis of the inorganic core, functionalization processes to make IONPs biocompatible and also to target them to specific tissues or cells, and finally in vivo studies in animal models, with special emphasis on tumor models.

Keywords Magnetic nanoparticles · Iron oxide nanoparticles · Magnetic resonance imaging · Cancer · Diagnosis

The article is a part of the Topical Collection "Surface-modified Nanobiomaterials for Electrochemical and Biomedicine Applications"; edited by Alain R. Puente-Santiago, Daily Rodríguez-Padrón".

✉ Manuel Pernia Leal
mpernia@us.es

✉ María Luisa García-Martín
mlgarcia@bionand.es

[1] BIONAND - Centro Andaluz de Nanomedicina y Biotecnología, Junta de Andalucía-Universidad de Málaga, C/Severo Ochoa, 35, 29590 Málaga, Spain

[2] Departamento de Química Orgánica y Farmacéutica, Facultad de Farmacia, Universidad de Sevilla, 41012 Seville, Spain

[3] Networking Research Center on Bioengineering, Biomaterials and Nanomedicine, CIBER-BBN, Málaga, Spain

Published online: 07 May 2020

1 Introduction

Magnetic resonance imaging (MRI) is one of the main in vivo imaging modalities, along with positron emission tomography (PET), computed tomography (CT) and ultrasound imaging. MRI is the most versatile of all of these, being able to provide both anatomical and functional information with excellent image quality, and, most importantly, using non-ionizing radiation, which allows longitudinal studies to be performed without the risk of side effects. The MRI signal comes from the radiofrequency signal of protons magnetized by an external magnetic field. These protons originate mainly from water molecules. The application of radiofrequency pulses is used to excite the magnetization, and magnetic field gradients are used to provide spatial localization. Contrast in MRI reflects differences in signal intensity, which depends on the concentration of water molecules within the tissue, the relaxation times, T_1 and T_2, of the water protons and the mobility of the water molecules (diffusion, flow) [1]. Additionally, image contrast can be further enhanced using contrast agents (CAs), with Gd-chelates being used most commonly in clinical practice. However, CAs lack specificity and have recently been related to toxicity issues caused by the unexpected release of free Gd. Magnetic nanoparticles have emerged as a promising alterative with improved properties in terms of specificity and biocompatibility. Over the past two decades, many studies have aimed at the development of new magnetic nanomaterials that can serve to improve the diagnosis and treatment of many different diseases. Among these nanomaterials, iron oxide nanoparticles (IONPs) have been investigated most extensively as CAs for MRI due to their magnetic properties, that is, the superparamagnetism that leads to very high relaxivity, their high biocompatibility, since they can be incorporated into iron metabolism, and also the easy functionalization of their surfaces with target molecules for molecular imaging purposes [2].

The first step in the development of IONPs is synthesis of the magnetic core, for which many different methods have been proposed, all aiming at strict control of the size, shape and magnetic properties, so that the synthesis process can be performed under highly reproducible conditions, which is one of the essential requirements for the potential clinical translation of these new nanomaterials [3]. Functionalization of magnetic nanoparticles is then needed to make them soluble in aqueous media and to provide them with stability and biocompatibility [4]. Further functionalization may include the addition of different molecules to target specific tissues or cells [5]. The most relevant functionalization strategies will be discussed in detail in this review. Finally, the in vivo characterization of IONPs is the most critical aspect in the development of IONPs for biomedical applications. Although many new nanomaterials show excellent in vitro properties, most of them fail when tested in vivo. Thus, around 6500 studies (PubMed database) on magnetic nanoparticles have been published since 2010, in which IONPs often appear as promising new CAs for MRI. However, up to now, extremely low clinical translation has been achieved [6]. Therefore, comprehensive studies with appropriate in vivo experimental models are of paramount importance for the successful development and eventual clinical translation of these nanomaterials.

In this review, we describe the recent advances in regard to the synthesis, functionalization and in vivo applications of IONPs as MRI CAs for the diagnosis of several pathologies, with special emphasis on cancer diagnosis.

2 Methods for the Synthesis of IONPs

Over the past few decades, various procedures to synthesize IONPs have come to fruition. The ultimate goal of these procedures is to gain complete control over the properties of IONPs, such as size, shape, saturation magnetization, etc. However, this has not yet been achieved completely. The main hindrance behind this failure is the inability to fully determine the science behind the processes and their mutual interactions, but it is not so distant in the future that we will be successful. Figure 1 shows different methods to synthesize IONPs, which are described in detail below, along with their pros and cons.

2.1 Coprecipitation

Coprecipitation is the method most commonly used for the synthesis of IONPs due to its facile nature. Massart [7] pioneered the existing scientific knowledge established by Le Fort [8] and Elmore [9] regarding the synthesis of magnetic colloids, and stressed the importance of the stoichiometric ratio between Fe(II):Fe(III) being 1:2. The synthesis process described by Massart requires the addition of alkaline medium (pH ~ 11, slowly or rapidly) into the iron salts solution at room temperature or at elevated temperature. This mixture requires an inert atmosphere to prevent nanoparticles from oxidizing. It was later established that the synthesis of particles follows the LaMer's model of nucleation and growth [10] (Fig. 2). The synthesis process has been described to occur in two steps, as shown below [11–14]

$$Fe^{2+} + 2Fe^{3+} + 8OH^{-} \leftrightarrows Fe(OH)_2 + 2Fe(OH)_3 \rightarrow Fe_3O_4 \downarrow + 4H_2O.$$

However, Lagrow et al. [15] recently challenged this mechanism of synthesis. They claimed that while increasing the pH via sodium carbonate, two intermediate phases are formed, one poorly crystalline ferrihydrite and another crystalline iron hydroxide carbonate. This ferrihydrite eventually grows into iron oxide at the cost of iron hydroxy carbonate. Even though Lagrow's proposed mechanism seems to answer a few loopholes undescribed by Massart, improving the homogeneity and reproducibility of the nanoparticles, it fails to ascertain if the same mechanism is followed when ammonia or ammonium hydroxide is used.

Irrespective of the mechanism followed, nucleation is judged as the size-determining step and is exploited to modulate the size of particles [14–16]. The nature of particles depends on various other factors, such as the type of salts used (e.g. chlorides, sulfates, nitrates, perchlorates, etc.), the Fe^{2+} and Fe^{3+} ratio, pH and the ionic strength of the media, along with the reaction environment [17–30]. Jiang et al. [24] showed that the particle size distribution is narrowed

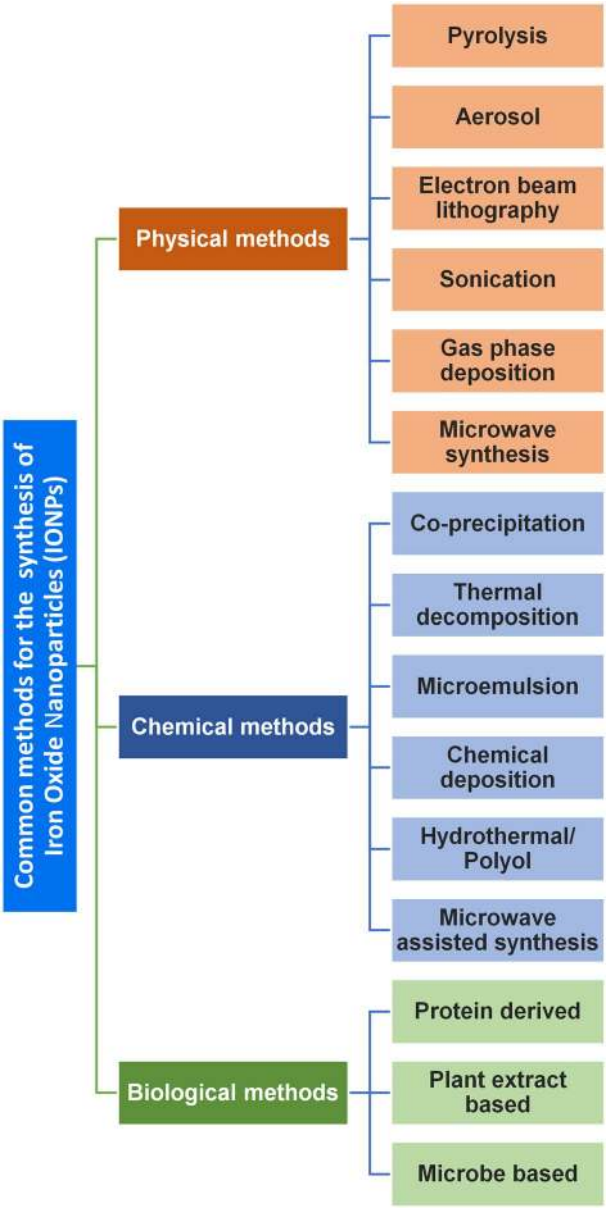

Fig. 1 Methods used in the synthesis of iron oxide nanoparticles (IONPs)

if the homogeneity of pH within the solution is improved by adding urea to the reaction mixture. There are also reports suggesting that particle size decreases with increasing pH [17]. A similar trend is observed between particle stability and iron concentration, but substantial studies are lacking to support this observation [23]. Particles with different morphologies, such as nanodots, ellipsoid,

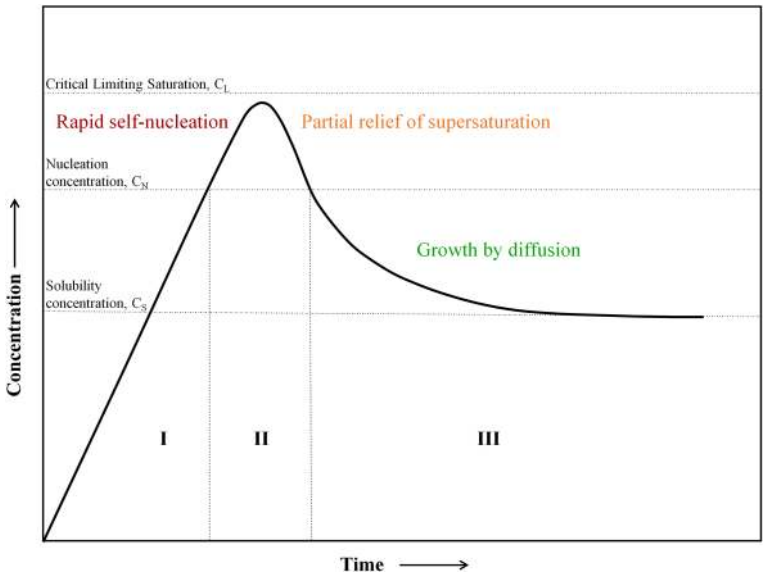

Fig. 2 LaMer's model depicting the nucleation and growth process of the nanoparticles. Adapted with permission from [10]. Copyright (1950) American Chemical Society

spherical, clusters or necklace like, can be synthesized by varying their aging conditions [25–27]. Itoh et al. [26] synthesized ellipsoidal and spherical hematite nanoparticles by aging them in phosphate ions and nitriloacetic acid (NTA), respectively. The relationship between shape/size and the electrostatic surface density of particles is linked to the interfacial tension between the oxide and the solution, which causes a decrease in the surface energy, thus modulating shape and size [28]. If a modern method like ultrasonication is used with coprecipitation, it can yield narrowly distributed particles, as shown by Bui et al. [31], who compared their modified version of the coprecipitation method (using ultrasonication instead of stirring) to the solvothermal method, and found the former to yield more homogeneous and small sized nanoparticles. However, the comparison between their method and the conventional coprecipitation method (with stirring) is missing. The major advantages of the coprecipitation method are its time saving facile nature, with no requirement of high temperature or pressure, and the production of particles with high yield and easily scalable to large quantities. However, the particles synthesized with this method generally lack homogeneity and form single and also multicore nanoparticles. Particles thus synthesized also tend to form aggregates, which leads to an undesired assortment of blocking temperatures. Another disadvantage of this method is that the pH of the resultant solution is too high, thus requiring neutralization before they can be used for biological applications.

2.2 Thermal Decomposition

In this method of synthesis, high temperatures are exploited to break down the precursor to yield nuclei as well as their further growth into nanoparticles (Fig. 3). It started as a way to ease the study of properties of systems with narrow size distribution [32]. Smith and Wychlk were among the first researchers who utilized this method to synthesize colloidal dispersions of iron using iron pentacarbonyl [$Fe(CO)_5$] as a precursor, along with different solvents and the addition of different polymers. They concluded that the polymers added during the reaction not only coated the dispersions forming stable particles, but also acted as catalysts for the decomposition [33, 34]. They suggested that the decomposition takes place at 140–160 ℃ in the presence of butadiene polymers while gathering support from the mechanistic studies conducted by Bergman and coworkers [35]. Later, their hypothesis was verified experimentally, showing the presence of an intermediate carbonyl complex formed after decomposition of $Fe(CO)_5$ [36]. The reaction takes place in two main steps: nucleation and growth. This separation of stages can be used advantageously to alter the size and shape of nanoparticles as demonstrated by Hyeon et al. [37] and Jana et al. [38]. They used iron oleate as precursor and proposed that nucleation starts at 200–240 ℃, initiated by dissociation of one of the three oleates available in one molecule of iron oleate [Fe-$(oleate)_3$], while the growth begins at 300 ℃ with the subsequent dissociation of the remaining two oleates. The complete mechanism of the reaction is not fully understood even though it has been widely studied, both experimentally and computationally [39–41]. Nonetheless, these studies led to the discovery of "polyiron oxo clusters" species as the actual precursor for the formation of nanoparticles, as initially suggested by Wells [36]. More recent studies have reported the synthesis of a new precursor by synthesizing an intermediate between $Fe(CO)_x$ and oleylamine (OLA), and achieved controllable size of 2.3–10 nm [42].

To date, different precursors have been reported in the literature: iron acetylacetonate [$Fe(acac)_3$] [43], iron cupferron [Fe(cup)] [44], iron chloride ($FeCl_3$) [45], iron pentacarbonyl [$Fe(CO)_5$] [46], along with different iron complexes such as iron oleate [45], iron stearate [38] and iron eruciate [47]. Depending on the process involved and the size required, it becomes important to select the right

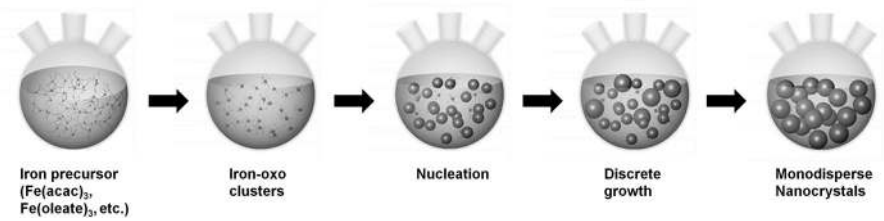

Fig. 3 Different stages during the synthesis of IONPs in the thermal decomposition method. Adapted and modified with permission from [41]. Copyright (2013) American Chemical Society

precursor as the reaction proceeds differently depending on the way the precursor is broken down [48].

There are several other factors that could affect the size and morphology of particles, such as temperature, nature of the solvent, reactants ratio, reflux time, and seed concentration [45, 49, 50]. Thus, Hyeon found that the heating rate of the reaction, along with the boiling point of the solvent used, is also a crucial factor to adjust the size of the nanoparticles [45], and Pellegrino's group concluded that there is an inverse relationship between the size of the nanoparticles and the heating rate [49]. However, controversy still exists regarding the role of the temperature ramp in the synthesis of IONPs, and, therefore, comprehensive and deeper studies are still needed to properly elucidate the mechanism involved.

Kovalenko et al. [51] showed the importance of surfactants, not only to prevent aggregation, but also to modulate shape and size. They displayed the use of fatty acids, such as oleic acid (OA) or salts of OA, to synthesize spheres and cubic nanoparticles, respectively. Later, several groups have tried to shed light on the role of OA as well as other fatty acids regarding the size and shape of IONPs, but up to now, a fully elucidated theory is still lacking [52–59]. Quality of particles can be further improved by the controlled addition of water and oxygen in the inert environment to decrease crystal defects, and improve magnetic properties and homogeneity [60, 61].

In summary, thermal decomposition, albeit a bit complex and time-consuming, yields very homogenous and monodisperse nanoparticles, making it one of the most used methods to synthesize nanoparticles for biological applications. The shape and size of nanoparticles can be controlled by tuning the parameters described above. Major drawbacks of this method include the inability to properly scale up and the lack of dispersibility of the particles in aqueous solvents, although this can be remedied by surface modifications in situ, as described by Li et al. [56, 62], or using post preparative methods, as explained in greater detail in later sections of this review.

2.3 Hydrothermal and Solvothermal Synthesis

In this method, the hydrolysis and oxidation (or neutralization) reaction takes place in a reactor or autoclave at high temperature and pressure. Depending on the reaction solvent, it is either referred to as hydrothermal (if the solvent is water) or solvothermal (any other solvent or combination). Both reactions follow the aforementioned model of nucleation and growth [63, 64]. There have been several reports [4, 37, 65–68] on the use of this method to synthesize magnetic nanoparticles as well as its comparison with other methods [69].

The reaction parameters, such as temperature, reactor size, time, concentration of the reactants, and the nature of the solvent and capping agents, affect the size, shape and other properties of the final product. Out of all these parameters, the effect of the solvent has been studied the most [70, 71], closely followed by that of the surfactant [72, 73]. The particles show a preferential surface binding towards the carboxylate from the OA rather than the amine from the oleylamine [72], which very likely is the case for every method described in this article, although it still needs verification.

This preferential binding was recently used by Brewster et al. [73] to present a new way to control the particle size and crystal phase. They varied the carbon chain length in the iron carboxylate, which was used as the precursor, and showcased the effect of two different ligands, amine and carboxylic acid, which were added to the reaction [73]. They demonstrated that the size of the particles decreased as the carboxylate chain length increased in the presence of amine ligands, while no definite trend was observed when varying the carboxylate free ligands.

The hydrothermal/solvothermal method has also been used to synthesize other ferrites [74]. Kim et al. [75] recently demonstrated a gram scale yield of magnetite nanoclusters by modifying the procedure and utilizing trisodium dihydrate, but, to the best of our knowledge, this is the only report for large scale synthesis using this method. To further exploit the particles thus formed for biological applications, surface coating becomes necessary, as will be discussed in detail in the subsequent section. Polymers such as polyvinylpyrrolidone (PVP), polyacrylic acid (PAA) and polyethanolimine (PEI), have been shown to improve the magnetic properties when used in the synthesis of monodispersed clusters [76]. Recently, Köçkar et al. [77] explained a way to get in-situ capping of IONPs with tartaric acid/ascorbic acid/ mixture of two, which led to the synthesis of uniform, un-agglomerated, biocompatible particles of less than 8 nm with good saturation magnetization. The hydrothermal/solvothermal method is, therefore, an ideal method for the synthesis of iron oxide nanoparticles, mainly nanoclusters. However, the main disadvantage of this method is that, due to the lack of stirring inside the autoclave, monodispersity, as well as scalability, can sometimes be hindered.

2.4 Polyol Method

This method is an iteration of the solvothermal method, with polyols being used as solvents to synthesize nanoparticles by dissolving the precursor, solubilizing in the diol at high temperatures, and eventually leading to the formation of metal nuclei and particles. Following previous works pertaining to synthesis of metallic powders [78–84], Caruntu et al. described this method to synthesize nanocrystalline metal oxide nanoparticles by synthesizing magnetite nanoparticles [85]. They explained the mechanism stating that reduction starts from the liquid state rather than the solid, and the nanoparticles are formed in two steps: hydroxides are formed first and then metal centers are chelated. Heterogeneous nucleation performs better than homogeneous nucleation as it has been studied to provide a better separation between nucleation and growth, thus giving better control over the size, shape and crystallinity [78]. Polyols play multiple roles, acting as reducing agent, stabilizer and solvent [86], modulating the process to yield large and small clusters [87], nanoparticles [88] or single-core/multicore nanoparticles [89]. Different polyols have been exploited for the synthesis of iron oxide nanoparticles, such as diethylene glycol, giving 3 nm particles [90], or triethylene glycol, giving 10 nm particles [91]. However, Cai et al. [92] reported that only triethylene glycol gives non-aggregated nanoparticles. To our knowledge, there are no reports on the use of tetra or penta ethylene glycol, which could have ameliorated the agglomeration problem

even more, if the trend described holds to be true. Other parameters that have been identified to modulate the size, shape, crystallinity and saturation magnetization are temperature, time, precursor concentration, and surfactant. The role of water was studied by Hemery et al. [93], when its importance was revealed by inability of the anhydrous iron chloride to produce magnetic particles [93]. The impact of stoichiometry in polyol synthesis has been studied by Wetegrove et al. [94], showing that the increase in Fe^{3+} concentration forms larger crystallites and the increase in Fe^{2+} content promotes nucleation [94].

As stated above, hydrophilicity is important, which is generally lacking in particles synthesized using the polyol method. However, there are reports of the synthesis of hydrophilic nanoparticles using this method [88, 95] but their limitations include the lack of a surface functionality for bioconjugation. This problem has further been remedied by the use of polyamines [96], polyimine with polyol [97], polyamine with polyol [98] and PAA [99]. The research done by Babić-Stojić et al. [100], wherein they esterified 3 nm IONPs in situ, implied the importance of the surface layer in the properties of nanoparticles.

The morphology of the particles is of equal importance as size in in vivo applications and has been shown to be altered by the addition of halide ions [101]. There have also been advancements in solvents, such as the thermostable ionic solvent [P6,6,6,14][Tf2N], which has been shown to be capable of synthesizing quasi spherical magnetite nanoparticles of around 14 nm [102].

In conclusion, the method described herein has the advantage of being environment friendly, scalable, and good for synthesizing both single and multicore particles. However, it has the drawback that the particles thus formed lack homogeneity.

2.5 Sol–Gel Method

This is a two-step chemical method, with the first step being the synthesis of the sol (particles in a solution) via hydroxylation of the precursors, and the second step, the formation of a gel by condensation and polymerization. Eventually, heat treatments are used to achieve a proper crystalline state. Costa et al. [19] were among the first to synthesize magnetic nanoparticles using this method, but they failed to identify the correct mechanism. Subsequently, the work of Portugal et al. [103], made the mechanism a bit clearer upon finding signatures of iron hydroxide, but the exact mechanism is still unknown. Like in the polyol method, the solvent is shown to affect the ferrite grain as well, but changes in grain size have been attributed to a different growth model with two different solvents [104]. Water concentration is also shown to improve hardness and structural defects [105].

Size and shape are also affected by other parameters such as solvent ratio, time, pH, stirring, gelating agent and, temperature. Liu et al. [106] used different calcination temperatures to synthesize different phases of IONPs, and this transformation has been attributed to two separate mechanisms, crystal regrowth and chemisorption, depending on the temperature. Akbar et al. claimed to have synthesized three different phases of iron oxide (α-Fe_2O_3, γ-Fe_2O_3, and Fe_3O_4) simply by varying the precursor to solvent ratio, thus suggesting the importance of that ratio [107]. The

particles were shown to possess higher saturation magnetization. They also observed differences in hematite particle size and morphology when using different precursors, with iron acetate giving rise to smaller spherical particles, while iron nitrate led to larger, quasi cubic particles. These differences were due to the water content as well as the presence of nitrate and carboxylate in the precursors [108]. More recently, Hu et al. [109] reported a new explosion-assisted sol–gel method in which they used ferric nitrate as precursor and citric acid as chelating agent to form a gel. The gel was then homogenized and heated with picric acid to attain highly pure, well dispersed and crystallized magnetite nanoparticles ranging from 3 to 20 nm. The synthesis was proposed to be resulting from the combined action of the complexing of citric acid with metal ions, and the explosion, thus explaining the important role of citric acid, not only as a carbon source, but also to allow the combustion and reduction of the dried gel simultaneously. The chemistry of the sol–gel method is vast, with the involvement of different precursors, gelators as well as chelators, but it is beyond the scope of this review. It is, however, nicely explained by Danks et al. [110].

This method is more recommended for synthesizing thin films [111] and nanocomposites [112, 113] since it can form thin films in just 2 min if the heating source is changed to microwaves, and pure phases can be formed by using high microwave power (600–800 W).

2.6 Microemulsion Method

The microemulsion method is a form of coprecipitation performed in a confined space such as micelles. It generally involves two immiscible liquids with surfactants forming the interfacial layer [114], and is classified as either the water-in-oil method or oil-in-water method [115]. Inouye et al. [116] were the first to report the synthesis of magnetic particles using this method, exploiting the faster oxidation of ferrous ions in micelles.

In water-in-oil microemulsion, a hydrophobic phase is used with aqueous droplets separated by a surfactant [117]. The most common surfactants used are PVP and cetyltrimethylammonium bromide (CTAB). In this method, particles generally collide and coalesce, and break again, leading to the growth of particles, the particle size being determined by the size of the droplets. In a final step, particles are centrifuged and lyophilized to get pure nanoparticles [118–120]. Many articles have been published on the use of this method to synthesize iron oxide nanoparticles [121–124]. Although surfactant concentration is not shown to affect the size, precursor concentration and temperature are important influencers, together with pH [125] and the choice of surfactant [126, 127]. Recently, Singh et al. [128] showed the importance of ionic concentration and temperature on the morphology, size and crystallinity by claiming that, in order to obtain monophasic particles, $[Fe^{2+}]$ and $[Fe^{3+}]$ should be ≤ 0.09 M and ≤ 0.184 M, respectively, with a temperature range of 65–72 ℃. They also observed changes in the morphology of the particles, from cubes to pentagons to spheres, when increasing the concentration of the surfactant (CTAB) between 0.01 and 0.1 M, but they did not describe

the mechanism, or explain why the shape of the CTAB nanodroplets changes upon varying concentration. Nor did they explain why particle size changed with concentration [128]. Bonachhi et al. [129] achieved ultra-small magnetic nanoparticles by using γ-cyclodextrin by hydrolyzing Fe^{2+} ions in aqueous solution, while Lee et al. [130] varied the ratios of the precursor and solvent from 3.6 to 8.1, and achieved 2 to 10 nm magnetite particles. Vidal et al. showed the importance of oleylamine as surfactant to prevent aggregation [131], while Pileni et al. explained the importance of using functionalized surfactants and pH to improve the crystallinity and morphology of the nanoparticles [132]. Following a similar approach, Han et al. used a nonionic surfactant, $C_{16}E_{15}$, to synthesize nanoparticles with high saturation magnetization (74.8 emu/g) [133]. It is worth mentioning that if the surfactant described in this method is replaced by a phospholipidic molecule to form particles within liposomes, they are termed magnetoliposomes, which show significantly higher blood half-life [134–136]. However, if the particles are formed within the aqueous compartment, they are known as magnetovesicles. These special particles can be synthesized using film hydration and extrusion [137], sonication [66], phase evaporation [138] and nanoreactor [139], and are very promising for biomedical applications.

Recently, even metallosurfactants have been used as precursors to synthesize particles of around 3 nm [140]. This method has also been utilized in exchanging the capping of iron oxide nanoparticles to improve solubility [141–143].

Similarly, oil-in-water has a hydrophilic solution with oil droplets used as a reactor. Recently, spinel ferrites have been shown to be synthesized using this method, with metal ethylhexanoates as precursors and a pseudo ternary solvent system, which includes oil, surfactant and water in the ratios of 20:20:60 [144]. The oil in water method has also been used as a strategy to cap nanoparticles [145].

The microemulsion method has several advantages, such as providing a narrow range of particles with relative ease, good morphology and without the need for high temperatures. But it also has disadvantages, including scalability, the toxicity of some surfactants, the amount of surfactant used, as well as the need for ligand exchange.

2.7 Aerosol Method

This is also a chemical method, which leads to high production of particles. This method can be subdivided in two categories. The first is spray pyrolysis, in which precursor salts are sprayed into the reactors, where they are condensed and solvent is evaporated, which in turn also means that the size of the particles depends on the droplets [146].

Serna's group [147] were among the first to synthesize Fe_2O_3 nanoparticles using this method. Their study claimed that if small size is the most important feature for the application, iron acetylacetonate should be used because of its exothermic decomposition reaction; however, if crystallinity is to be considered, then iron chloride is favored due to solvent elimination at higher temperature. This leaves other precursor benefits open for exploration. The importance of intraparticle reactions in controlling the size of particles was established later, along with the solvent, rate

of evaporation, time spent in the reactor, and temperature. These studies concluded that the heating time and temperature, along with the type of evaporation or reaction taking place during the drying stage, will conform the particle structure as hollow, dense, foam-like, etc. [148, 149]. Zheng et al. [150] recently reported that chloride ions prevent phase transition from γ-Fe_2O_3 to α-Fe_2O_3 at higher temperatures, leading to higher magnetization, which highlights the importance of chloride ions in the reaction. Das et al. proposed a new strategy to decrease size with high crystallinity by adding ethanol to the ultrasonic pyrolysis [151]. It was explained that the faster evaporation rate of ethanol compared to water, as well as a decrease in surface tension of the water–ethanol solution, led to the formation of smaller droplets and eventually smaller particles. Since the rate of evaporation of the solvent has been stressed and linked to particle size, it might be interesting to see how methanol, or any other solvent with a boiling point lower than that of ethanol, affects the size and crystallinity of particles.

The second category is Laser pyrolysis, a gas phase method that utilizes the heat generated by a laser to heat the precursors and the flow of a gas or a mixture of gases to produce nanoparticles. The sizes of the particles can be controlled by modulating the power of the laser since a direct relationship exists between the two [152, 153]. Zhao et al. [154] were the first to improve on the TEA laser using a cw CO_2 laser, which yielded particles with higher purity. There have also been reports on use of this method to synthesize hybrid silica-iron oxide composites [155]. Laser pyrolysis has a new iteration, flame spray pyrolysis (FSP), which uses a flame to heat the precursor [156]; the size of the nanoparticles can be controlled by varying the flame length or the oxidant flow rate, and the precursor/fuel composition. Lower flow rate of the oxidant leads to reduced flame length, with higher temperatures thus forming smaller particles and vice versa [157].

The main advantage of this method is that it helps in achieving very high homogeneity and monodispersity irrespective of the complexity of particles, including hybrid silica-iron oxide composites [155].

2.8 Sonochemical Method

This method utilizes acoustic cavitation, which means the formation, growth and collapse of bubbles generated by ultrasound, to synthesize nanoparticles. Instead of using high temperature or pressure directly, this method creates them indirectly by using bubbles or cavities formed in the liquid by the acoustic waves. Further oscillation of such waves helps them gather and store ultrasonic energy, creating a hot spot (~5000 K) and leading to the synthesis of particles of different shapes and sizes. This method works for both volatile and non-volatile solvents [158–160]. The reaction medium was already considered the most important factor in controlling the properties of nanoparticles by Suslick et al. [160] when they proposed the method, since the bubbles formed will depend on the vapor pressure of the media. The nature of the particles can also be altered by changing the ultrasonic frequencies based on the inverse relationship between oxidation of Fe^{2+} to Fe^{3+} and ultrasonic frequencies

[161]. The synthesis of particles in the presence of different ligands has also been performed, giving rise to particles between 5 and 16 nm [162].

Vijayakumar et al. [163] used a similar route to synthesize IONPs. They proposed a mechanism stating that ultrasonic waves produce the vaporization of water and further pyrolyzation into H and OH radicals due to prolonged temperature and pressure, which leads to the formation of hydrogen (H_2) and hydrogen peroxide (H_2O_2) from the reaction between H_2 and hydroxyl radicals, respectively. Meanwhile, the same energy also breaks down iron acetate into Fe(II) ions. These Fe(II) ions are later oxidized to Fe(III) using H_2O_2 as oxidant and forming Fe_3O_4 by using OH radicals [163]. There are several studies showing the effect of surfactants on the particles. Mukh-Qasim et al. [164] used SDS as stabilizer to get around 8.5 nm amorphous but water dispersible Fe_3O_4 particles, while Rahamwati et al. used iron sands along with different concentrations of PEG-6000. This latter group showed that, as PEG concentrations increased, the crystallite size of the particles increased [165]. They also showed that the morphology of the particles shifted from flower-like to cubes to spheres with increasing PEG concentrations. Kim et al. [166] synthesized OA-capped IONPs, which form a ferrofluid when dispersed in chitosan, with a hydrodynamic diameter of 65 nm, thus being potential MRI CAs. This method can also be used to synthesize composite nanoparticles [167] or other ferrites [168, 169].This method has also been used for surface functionalization in very short time [170].

The main advantage of this method is its accelerated nature to produce nanoparticles with good yield, but it falls short when it comes to phase homogeneity.

2.9 Microwave Synthesis

This is a modern-day hydrothermal method of synthesizing nanoparticles and one of the most used in recent days due to its much-improved kinetics of crystallization. It requires as low as 10 s and yields small and monodisperse particles due to homogenous heating [171].

Palchik et al. were among the first to use this method in a domestic microwave oven and suggested that the synthesis of particles was happening due to thermal breakdown of $Fe(CO)_5$, which in turn was taking place due to heating of chlorobenzene, since $Fe(CO)_5$ is a microwave resistant compound [172]. This indirectly marks the importance of the solvent. On the other hand, Liu et al. demonstrated the importance of water in maintaining a stable heating environment, along with the role of stoichiometry [173]. Another important parameter that have been studied extensively is the nature of the surfactant, with studies reporting the use of different concentrations of OA [174], amino acids [175], polyethylene glycol (PEG) [176], and different ratios of OA and oleylamine (OLA) [177]. OA is shown to increase saturation magnetization with increasing concentration, with no definite trend in size. However, concentrations beyond 0.35 mmol/dm^3 led to agglomeration and the product became difficult to isolate. Recently, amino acids such as glycine have been shown to reduce the crystallite size of IONPs, opening the path to explore other amino acids [175]. The presence of PEG in the reaction has also been shown to lead to smaller IONPs,

as compared to the reaction in its absence. When the reaction is performed in the presence of PEG, it tends to favor the formation of magnetite instead of maghemite. This happens due to PEG being sacrificial in nature and thus preventing oxidation. High microwave power and low synthesis time also favors the formation of maghemite [176]. Other studies have shown that the presence of OA during the synthesis, along with OLA, reduces aggregation among particles [177]. Temperature has also been shown to transform phases in IONPs [178]. Blanco-Andujar et al. proposed a facile method to synthesize citric acid coated IONPs and potentially scale them up [179]. The importance of aging temperature on crystallinity can be seen when Fe_2O_3 nanocubes are synthesized by decomposing iron oleate in a microwave and aging it in an autoclave at 180 ℃ for different time intervals [180]. Particles aged for 20 h showed cubic shape and higher saturation magnetization. Hu et al. [181] argued that the precursor is the most important parameter by synthesizing three phases of iron oxide, hematite, magnetite and maghemite, using $FeCl_3$ alone or in combination with $FeCl_2$.

Literature suggests that the morphology and composition of the particles can also be controlled using this method. Different morphologies, such as lamellar sheets [182], octahedrons [182] and hexagonal plates [183] are synthesized by slight changes in salts. Cu-doped IONPs with good colloidal stability are obtained in 10 min [184] using the microwave method. In fact, even using a domestic microwave, sizes of 8–10 nm can be easily achieved [185].

This method has been shown to be better than hydrothermal [186] or thermal decomposition [187] in terms of size, crystallinity and saturation magnetization. However, particles thus synthesized display lower surface reactivity than those synthesized using the thermal decomposition method, although with more ease of stabilization. The versatility of this method is acknowledged by its association with different methods: coprecipitation [179], thermal decomposition, [177] polyol [188] and sol–gel methods [189]. The particle size can be varied by modulating the power and hence the temperature, the time spent in the reactor, the cooling rate, etc. This method has become more popular recently due to its multiple advantages.

2.10 Biosynthesis

This is an eco-friendly method as most of the constituents needed are available from nature directly or indirectly. It generally involves the use of microbes [190] or plant extracts [191] to synthesize nanoparticles. Lovely et al. [192] were the first to use a microbe, GS-15, to form magnetite nanoparticles. Thereafter, many different magnetic bacterial strains were found and studied in order to produce IONPs [193–197].These nanoparticles are formed by the reduction/hydrolyzing capabilities of these biological entities. However, when a bacterium is used, its nature as well as its incubation time becomes an important parameter since it allows changes in size and morphology [198, 199]. Even fungi such as *Fusarium oxysporum* and *Verticillium* sp., have been shown to possess hydrolyzing capabilities to form different sizes and shapes of nanoparticles [200]. Viruses such as tobacco mosaic virus (TMV) have also been used as templates to synthesize nanotubes [201]. Iron oxides formed by microbial reduction have been

shown to lead to phase transformation with better crystallinity, although decreasing their reducibility [202].The scalability issue has also been answered by using a 30-l reactor, although there is only one report of such nature [203].

Plants or plants extracts have been used for the synthesis of nanoparticles [204]. Most recently, IONPs have been synthesized using figs, *Ficuscarica* and *Plantago major* extracts, which, apart from reducing precursors, also cap and stabilize the particles. These reactions have been concluded to take place due to the presence of phenols, and normally lead to sizes ranging from 2 to 50 nm [205, 206].

The main advantages of this method are that it is energy saving and non-toxic. Also, there is an unlimited supply of reducing agents, making it economically viable. On the other hand, its major disadvantage is unpredictability regarding the nature of the particles, with less control over the shape and size, along with uncertainty of yielding monodisperse particles when scaled up.

2.11 Other Methods

Several different methods for the synthesis of IONPs have not been described above due to a dearth of information in the literature. Alvarez et al. [207] developed a novel flow injection synthesis (FIS) method to fabricate magnetite nanoparticles in a capillary reactor, and produced homogenous particles of 2–7 nm with high reproducibility. There have been reports of the use of metal rods as anodes and electrochemical deposition in the presence of surfactants to yield 3–8 nm particles [208–210]. Chemical vapor deposition (CVD) [211, 212] has been used to fabricate thin films and morphology-controlled nanoparticles. Other methods, such as synthesis in a reactor [213], the solution combustion method [214], and the use of microfluidic channels on a chip [215, 216], have also been introduced.

All the methods described above have their own pros and cons, and the choice of one or the other depends on the application for which the nanoparticles are being developed. Thus, for nanoparticles to be used as MRI CAs, the most suitable methods appear to be the thermal decomposition or microwave methods, since they provide a very narrow size distribution, high saturation magnetization and good morphology control.

3 Functionalization of IONPs

One of the most important topics in the design of IONPs for in vivo applications is functionalization, which provides NPs with high stability in physiological media, stealth and vector targeting properties. In this section, we summarize the most relevant methods to functionalize IONPs for clinical purposes.

3.1 Organic Supra-structures

In recent decades, a class of highly branched and monodispersed macromolecules with well-defined three-dimensional (3D) architectures, such as nanomicelles,

dendrimers, liposomes and nanogels, have been developed to create hybrid nanoscale materials for imaging and therapeutic applications.

3.1.1 Nanomicelles

Nanomicelles are formed by the self-assembly of surfactant molecules or copolymers that adopt a core–shell like structure, thus entrapping in their inner core hydrophobic materials, such as drugs, dyes or inorganic nanoparticles (Fig. 4). The small size is another advantage of the micelles, which can be synthesized between 5 and 100 nm. This provides nanomicelles with long blood circulation times, which favor their active or passive accumulation in the target sites. Consequently, nanomicelles are generating great interest in the development of promising payload nanocarriers for theranostics [217–219]. Particularly interesting are the results obtained with hybrid nanosystems using polymer micelles loaded with IONPs. For instance, Jianping Bin and coworkers described the synthesis of a tumor-targeted MRI vehicle through the encapsulation of IONPs in self-aggregating polymeric folate-conjugated *N*-palmitoyl chitosan micelles [220]. In vitro and in vivo studies demonstrated the efficacy of folate-conjugated superparamagnetic iron oxide nanoparticle (SPION)-micelles in targeting and visualization by MRI of folate receptor overexpressed tumor cells. Torchilin et al. [221] created a diagnostic and therapeutic agent for in vivo use based on poly (ethylene glycol)-phosphatidylethanolamine (PEG-PE) micelles loaded with Paclitaxel (PTX), a poorly water soluble anticancer drug, and IONPs. The combination of both multi-modal cargos inside the micelles showed no property changes, either in the relaxivity of the IONPs or in the apoptotic antitumour activity of PTX.

3.1.2 Dendrimers

Dendrimers are a class of well-defined nanostructured macromolecules consisting of three critical architectural domains: the multivalent surface, the interior shells surrounding the core, and the core. These domains can be tailored for a specific

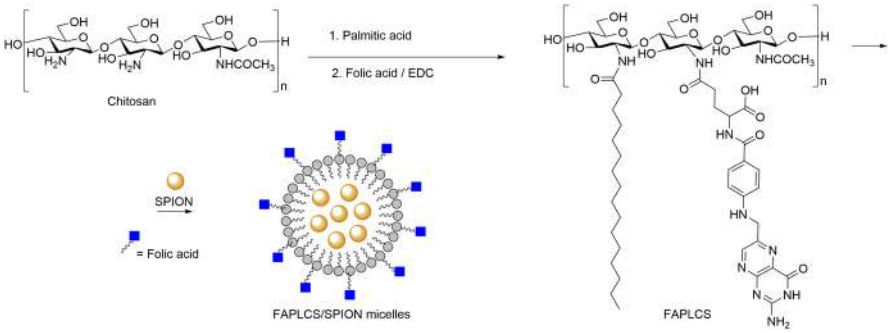

Fig. 4 Synthesis of chitosan derivative polymeric micelles encapsulating superparamagnetic iron oxide nanoparticles (SPIONs) [308]

purpose, such as a dendritic sensor [222, 223] or a payload carrier, the encapsulation of molecules in their interior shell being the most used application of dendrimers [224, 225]. One of the most common dendrimers is based on the chemical structure poly (amidoamine) (PAMAM), which has a large number of reactive amine groups on the periphery, making them an excellent platform to construct nanomaterials for biomedical applications [226–228]. Luong et al. [229] designed a promising theranostic agent based on the combination of IONPs and a hydrophobic anticancer drug loaded in a PAMAM dendrimer decorated with folic acid (FA). The design of this hybrid theranostic agent starts with functionalization of the SPIONs with activated carboxyl groups that bind folic acid-PAMAM dendrimers. The engineered SPIONs@FA-PAMAM showed great potential as MRI diagnostic agents, with increased internalization in cancer cells and better image contrast. Moreover, the encapsulation of hydrophobic anticancer drugs, such as 3,4-difluorobenzylidene-curcumin (CDF), in the dendrimers of the SPIONs@FA-PAMAM, enhances their anticancer activity by delivering a higher dose of CDF with high specificity to target cancer cells expressing folate receptors.

Dendrimers could also be used in gene therapy as gene delivery platforms. Xiao et al. [220] synthesized a nanohybrid dendrimer based on the combination of PAMAM dendrimers and IONPs through electrostatic interactions. First, the IONPs were functionalized with negatively charged polystyrene sulfonate (PSS), and then positively charged PAMAM dendrimers decorated with plasmid DNA were deposited onto the PSS-functionalized NPs, resulting in a nanohybrid material, PAMAM dendrimer/pDNA-coated MNPs. The results demonstrated that the efficiency of this hybrid system to transfect NIH 3T3 cells is strongly dependent on the dendrimer generation, the amine/phosphate groups ratio and the plasmid DNA concentration.

3.1.3 Liposomes

Liposomes comprise a lipid bilayer surrounding an aqueous core. They can be made from different lipid formulation and present different sizes depending on the method of preparation. Similarly to the organic macro-structures mentioned above, liposomes are able to encapsulate payloads in their hydrophobic or hydrophilic inner, which makes them excellent nanocarriers for therapeutic and imaging applications. Liposomes based on phospholipids are the most common vesicles for in vivo applications due to their great advantages, such as biocompatibility, biodegradability and reduced toxicity [230–232]. The incorporation of IONPs into liposomes is gaining increased attention of researchers as a way to synthetize more effective magnetic nanocarriers for in vivo applications. Di Corato et al. [233] designed a liposome formulation based on phosphatidylcholine lipids that entraps magnetic NPs and a photosensitizer in its interior. In a single synthesis method, higher concentrations of hydrophilic IONPs were encapsulated in the core, and a hydrophobic photosynthesizer, Temoporfin (marketed as Foscan), was incorporated into the lipid bilayer. The resulting magnetic liposome presented double functionality, magnetic hyperthermia and photodynamic therapy, which led to complete death of cancer cells in vitro and total ablation of solid-tumor in vivo.

Zheng et al. [234] synthetized a tumor-specific peptide-decorated liposome containing payloads of IONPs and an anti-cancer drug in their inner core and lipid bilayer, respectively. Like the protocol described above, the combination in a single pot reaction of egg phosphatidylcholine, cholesterol, paclitaxel (PTX), different 1,2-distearoyl-sn-glycero-3-phosphoethanolamine (DSPE) phospholipids, such as DSPE-PEG and cell penentrating peptide-modified DSPE-PEG, and hydrophilic SPION, generated a theranostic liposome. The results confirmed the effectiveness for tumor targeting and anti-tumor activity through MRI in vivo experiments.

3.1.4 Nanogels

Nanogels (NGs) are nanosized water-soluble particles formed by crosslinked polymer networks with loading capacity of therapeutics. Stimuli-responsive NGs are a class of smart particles that respond to external physical changes, such as pH, temperature or redox agents [235, 236]. This behavior allows the controlled-release of payloads from NGs, minimizing possible side effects and avoiding the use of high doses. NGs can also be loaded with diagnostic agents, such as magnetic NPs, enabling their visualization and follow-up by MRI. These characteristics, together with the ease of uptake by cancer cells and tumor tissues due to their softness and fluidity, make NG-based nanosystems a high potential theranostic material [237, 238].

Qian et al. [239] prepared a hybrid NG system based on a thermo-responsive copolymer [*N*-isopropylacrylamide, methacrylic acid and poly (ethylene glycol) methacrylate] that stabilizes hydrophobic IONPs and 10-hydroxy camptothecin (HCPT) in its inner compartment. The obtained IONP/HCPT-NG generated an increase in reactive oxygen species (ROS), allowed the enrichment of NG at the tumor site by applying an external magnetic field, and offered the possibility of being used as nanocarrier for photothermal therapy due to its absorption in the near infrared (NIR) range. In vivo results demonstrated that the combination of PTT and chemotherapy with external magnetic fields on IONP/HCPT-NGs, reduced the growth of primary tumors and prevented metastasis [239].

Alginate (AG) is a natural polysaccharide that has been gaining attraction in recent years for the synthesis of polymeric nanomaterials with biomedical applications thanks to its biocompatibility, biodegradability and ease of gelation [240]. For instance, Hao et al. [241] designed alginate NGs loaded with IONPs and bone mesenchymal stem cells (BMSCs) for enhanced tumour MR imaging (Fig. 5). The potential advantage of using BMSCs as tumor delivery vehicles is that they are not tumorigenic and minimally immunogenic. In this way, polyethilenimine (PEI)-functionalized IONPs were crosslinked to AG NGs previously synthesized by a double emulsion method. The resulting AG/PEI-NP NGs were taken up by BMSCs without affecting cell characteristics. BSMC-AG/PEI-NP NGs were then used successfully for the in vivo diagnosis of different tumor models [241].

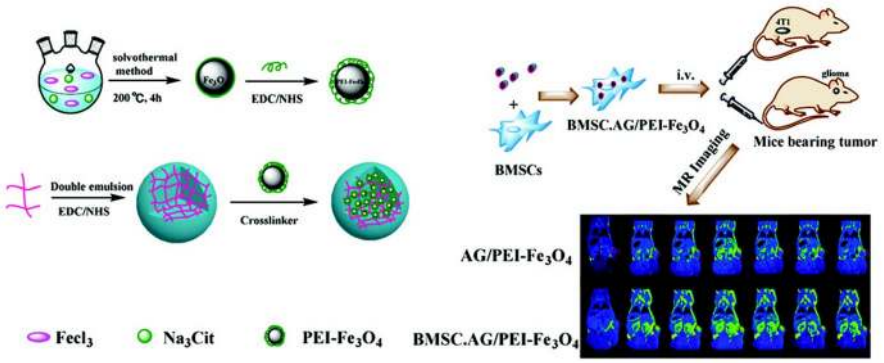

Fig. 5 Schematic illustration of alginate/polyethilenimine-iron (III) oxide (AG/PEI-Fe_3O_4) and stem-cell-mediated delivery of nanogels (NGs) for enhanced breast or glioma tumor molecular resonance (MR) imaging. Reprinted with permission from [241]. Copyright (2019) Royal Society of Chemistry

3.2 Inorganic Coverage

Mesoporous silica is the most important inorganic coating material for IONPs due to the ease of functionalization, high stability, and vast surface area and pore volume to host large number molecules. These characteristics make hybrid mesoporous silica-IONPs excellent nanocarriers for controlled drug release therapies [242, 243].

Based on this, Vallet-Regí et al. [244] designed a responsive silica matrix nanocarrier for tumor therapy based on magnetic NPs that combine the heat release mediated by magnetic hyperthermia and doxorubicin release through a thermoresponsive polymer. The as-prepared OA-capped IONPs are transferred into aqueous solution with CTAB, which helps the growth of the silica matrix by addition of tetraethyl orthosilicate (TEOS) as a silica precursor. Then, the silica-matrix-coated IONPs are functionalized with a methacrylate molecule as a polymer precursor to perform, using *N*-isopropylacrylamide (NIPAM), *N*-(hydroxymethyl)acrylamide (NHMA), and *N*,*N*′-methylenebis(acrylamide) (MBA) monomers, the synthesis of a thermoresponsive polymer surrounding the mesoporous silica-coated IONP (Fig. 6). Direct injection into the tumor site of Doxo-loaded mesoporous silica NPs, together with the application of amplified magnetic fields, provoked a synergistic effect between magnetic hyperthermia and chemotherapy that led to significant tumor growth inhibition and low toxicity [244].

Hurley et al. [245] demonstrated that the inclusion of functionalized mesoporous silica coating in IONPs cores results in stable NPs with high heat capacity and high MRI contrast. The anionic surfactants capped IONPs (a commercially available IONP called EMG-308) required pre-functionalization with polyvinylpyrrolidone (PVP) prior to silica condensation with the TEOS precursor. Finally, the functionalization with PEG and trimethyl silane derivates yields colloidal stable NPs with the same magnetic character that un-functionalized IONPs and minimal toxicity toward human skin fibroblasts. Furthermore, a direct injection into LNCaP prostate cancer tumours implanted in nude mice showed that these hybrid mesoporous silica-IONPs can improve the heating and imaging contrast of IONPs [245].

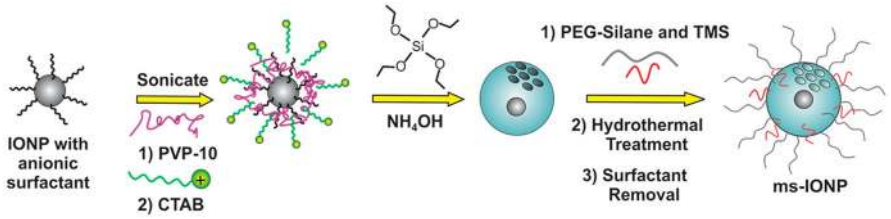

Fig. 6 Synthesis of mesoporous silica-coated (ms)-IONPs. Polyvinylpyrrolidone (PVP)-10 was added to IONPs prior to cetyltrimethylammonium bromide (CTAB) addition and silica condensation to allow for CTAB colocalization with IONPs and to maintain a spacer layer between the silica shell and IONP core. Reprinted with permission from [245]. Copyright (2016) American Chemical Society

3.3 Ligand Exchange

Ligand exchange is a very complicated coating strategy that involves multiple interactions potencials/forces. It requires the use of reactive binding molecules that enable the replacement of capping agents attached to the nanoparticle surfaces. This binding between the iron atoms of the IONP and the anchor group of the ligand molecules is mediated by electrostatic interactions. Therefore, the nature of the anchor group is determinant in the search for highly stable ligand molecules at the IONP surfaces. In addition to anchor groups, the hydrophilic balance of the ligand is also important to render water-soluble NPs [236, 246, 247]. In our group, we have developed different ligand formulations to functionalize IONPs to obtain soluble and stable NPs in physiological media for in vivo MRI applications. These ligands are based on a gallol group as a strong binder and PEG chains as hydrophilic tunable spacers, which also minimize plasma protein adsorption. In this manner, we have demonstrated that selection of the right molecular weight of PEG chain and the outermost charged group of the ligand plays a fundamental role in the fate and bioavailability of intravenously injected IONPs. Thus, a ligand with a PEG chain between 1500 and 3000 Da and neutral outermost groups showed the best stealth properties, resulting in longer blood circulation times and higher bioavailability without increased toxicity [248–250].

4 Applications of IONPs in MRI

Among the main clinical diagnostic techniques, MRI stands out for its unique combination of qualities, such as its non-invasive character, the absence of ionizing radiation, excellent image quality, and its ability to provide both anatomical and functional information [251]. The MRI signal comes mainly from the protons of the water molecules, while the image contrast is generated from differences in the intensity of this signal among different tissues, which depends on the concentration, relaxation times (T_1 and T_2) and mobility of the water molecules within each tissue [252, 253]. Additionally, image contrast can be further enhanced using CAs. Although there are several mechanisms that can produce MRI contrast, such as

chemical exchange saturation transfer (CEST) or hyperpolarization, most MRI CAs produce contrast by altering the relaxation times of the surrounding water protons [254, 255]. The capacity of a CA to decrease the relaxation times (T_1 or T_2) is given by a parameter known as relaxivity (r_1 or r_2), which is expressed in $mM^{-1}{\cdot}s^{-1}$.

In MRI, among the most commonly used CA are chelates of paramagnetic gadolinium(III) ions (Gd^{3+}). However, conventional Gd-chelates have some important limitations, such as the lack of diagnostic specificity and the toxicity associated with their use as a result of the unexpected release of free Gd ions [256, 257]. Magnetic NPs have emerged as a promising alternative to overcome these limitations [258].

4.1 IONPs in Tumor Diagnosis

4.1.1 Untargeted IONPs

The evaluation of IONPs as CAs in cancer research is performed mainly in rodent models, called 'indirect xenografts' [259]. Cancer cells can be implanted either into a tissue unrelated to the original tumor site (heterotopic model) or into the corresponding anatomical position (orthotopic model) [260] (Fig. 7). The route of administration of magnetic NPs is also relevant as it influences the biodistribution and pharmacokinetics of the CA. Several administration routes have been used in preclinical studies, mainly intratumoral, intraperitoneal or intravenous injection; for obvious reasons, the latter is the most interesting for clinical applications. After intravenous administration, IONPs have been described to accumulate in tumors due to the EPR (Enhanced Permeability and Retention) effect. This passive transport is determined by the high vascularization of tumors, and therefore increased blood flow, together with increased vascular permeability and poor lymphatic drainage [261]. Efremova et al. [262] developed IONPs for diagnosis of breast cancer in a heterotopic model. They observed that IONPs accumulated passively inside the tumor 24 h after intravenous injection using T_2-weighted MR images. Similar studies have been conducted using orthotopic models of breast cancer [263, 264], pancreatic cancer [265] and glioblastoma multiforme (GBM) [266]. All these studies conclude that IONPs accumulated in the tumor due to the EPR effect; however, most of them lack quantitative analyses, which are necessary to determine the amount of IONPs that actually reach the tumor.

Intratumoral administration could be an alternative for tumor therapy when the CA is not able to reach the tumor by a venous route. However, this approach has serious limitations for diagnostic applications since, in most cases, it would not add any useful information to that already provided by the MR images without CA. Furthermore, intratumoral administration makes no sense when it comes to very early diagnosis, detection of metastasis or in the case of inaccessible tumors. Nevertheless, several preclinical studies have been conducted using intratumoral injection of IONPs [267–269]. The authors used qualitative MRI to evaluate the distribution of IONPs throughout the tumor, which showed that IONPs spread slowly and inefficiently. Therefore, in these studies the information provided by MRI after the

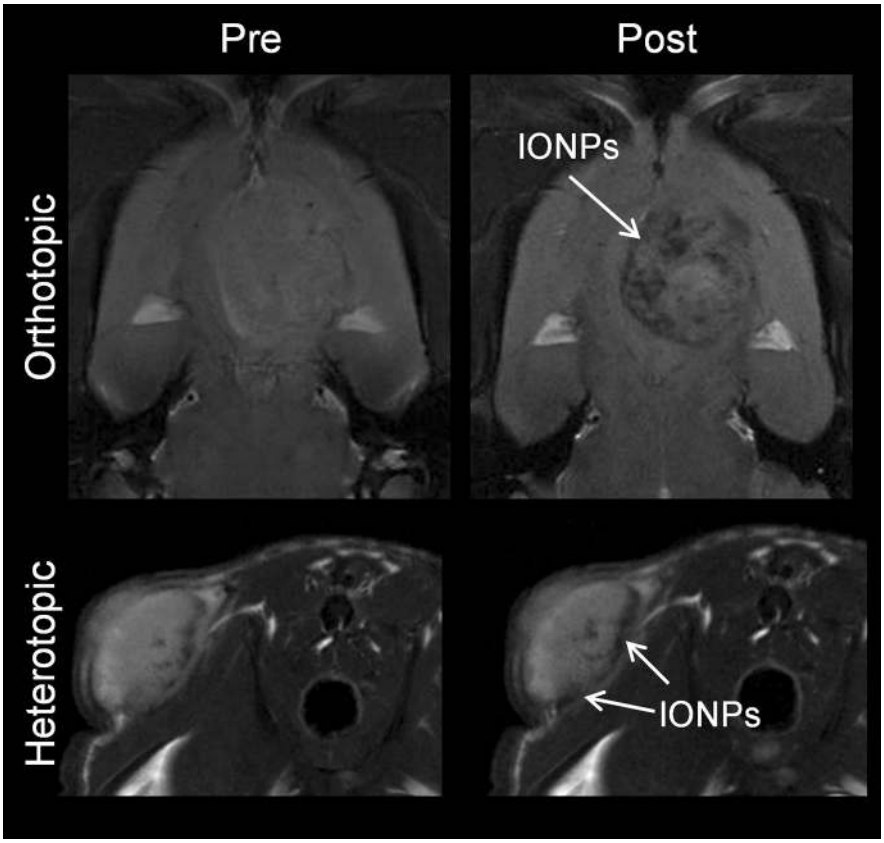

Fig. 7 C6 brain tumor model implanted orthotopically (upper panels) and heterotopically (lower panels). Left) T_2-weighted MR images before the injection of IONPs; right) T_2-weighted MR images 1 h after the injection of IONPs

intratumoral injection of IONPs serves as proof of concept, but, as we have just mentioned, it is of no practical value for potential clinical applications.

In conclusion, up to now, untargeted IONPs have not proven to be a good alternative to conventional MRI CAs for cancer diagnosis.

4.1.2 Targeted IONPs

To improve the accumulation of IONPs in tumors, a promising strategy is conjugation with targeting segments [5]. In principle, this functionalization would allow not only the visualization of IONPs by MRI, but would also offer the possibility of visualizing cellular and subcellular functions and processes in living organisms without perturbing them, giving rise to so-called molecular MRI (mMRI) [270], which was first described by Richard Klausner [271, 272] (Fig. 8).

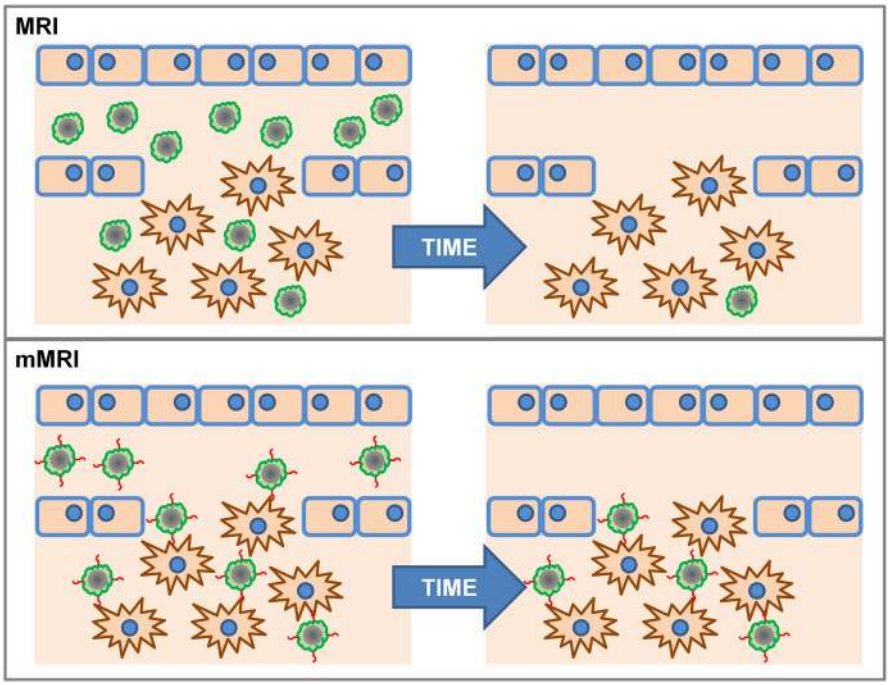

Fig. 8 Scheme of the non-targeted (top) and targeted IONPs (bottom)

It is worth mentioning that the targeted strategy for cancer diagnosis was described before the untargeted strategy. Reimer et al. [273] described in 1990 the diagnosis of liver cancer after the intravenous administration of IONPs-arabinogalactan conjugates, in both heterotopic and orthotopic models.

IONPs have been functionalized with epithelial growth factor (EGFR) antibodies for the diagnosis of breast cancer [274], pancreatic/stomach cancer [275] and brain cancer [276]. Because there is an established relationship between mutations involving overexpression or overactivity of EGFR and various types of cancer, this receptor is currently one of the most important targets in cancer research [277–279]. Similarly, PSCA (prostate stem cell antigen) antibody was bound to IONPs for diagnosis of prostate cancer [280].

Integrins receptor, especially $\alpha_5\beta_3$, has been found to be differentially overexpressed in tumors, playing a vital role in tumor angiogenesis [281–283]. Integrins are recognized mainly by short peptide sequences, such as Arg–Gly–Asp (RGD). Therefore, some NPs functionalized with RGD have been proposed for the diagnosis of brain cancer [284], colon cancer [285] or fibrosarcoma [286], among others.

Among other functionalization molecules for targeted diagnosis, it is worth highlighting the use of aptamers for kidney [287] and liver cancer [288], peptides for prostate and liver cancer [289, 290], and flavin adenine dinucleotide (FAD) for prostate cancer [291].

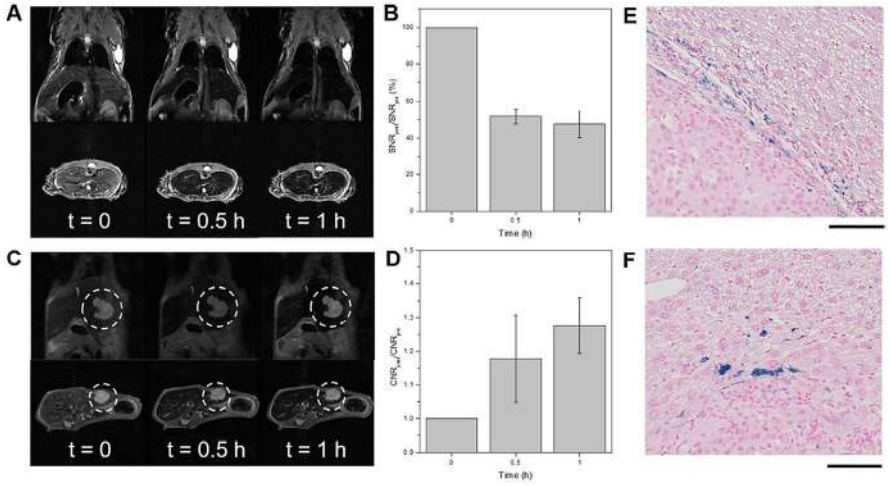

Fig. 9 **a** In vivo MR images of a NCr nude mouse at different time points after intravenous injection of IONPs. **b** Quantification of liver contrast collected at different time points after accumulation of IONPs in NCr nude mice. **c** In vivo MR images of liver tumor orthotopic xenographs at different time points after intravenous injection of IONPs. **d** Quantification of contrast-to-noise ratio (CNR) of tumor-to-liver contrast at different time points. **e**, **f** Histopathological analysis of mouse liver 1 h after the intravenous injection of IONPs. Reprinted with permission from [292]. Copyright (2018) American Chemical Society

Recently, Chee et al. published an interesting study in which they described the design of a library of short peptides and ligands to functionalize IONPs. From this library, they selected the ligand that provided IONPs with the best characteristics for in vivo use, namely, long term stability, non-specific binding to live cells and absence of cytotoxicity at high concentrations. IONPs functionalized with this ligand showed a significant increase in contrast between the liver tumor and the healthy liver tissue, as compared with commercial MRI CAs [292] (Fig. 9).

Finally, it is worth mentioning that, in clinical diagnosis, positive contrast is generally preferred over negative contrast because it avoids the potential confusion of signal decay caused by negative CAs with signal voids caused by magnetic field inhomogeneities induced by air, metal prosthesis, etc. Thus, a very recent study described the use of Cu as a dopant agent that enhances the positive contrast of IONPs functionalized with RGD for targeted diagnosis of breast cancer [184]. Even though many IONPs show dual contrast potential, that is, r_2/r_1 ratio between 3 and 10, their use in vivo as positive CAs is limited by the acquisition conditions of conventional T_1-weighted MRI sequences, which are usually based on the spin-echo acquisition scheme and therefore require relatively long echo times. However, the introduction of new MRI acquisition sequences, such as ultra-short echo time (UTE) sequences, is making it possible to detect IONPs as positive contrast [293].

4.2 IONPs as CA in Other Pathologies

Although most research in IONPs designed to serve as MRI CAs is focused on cancer diagnosis, there are many other pathologies that can benefit from advances in this field of research, as discussed henceforth. Recent investigations have demonstrated that an acetylcholine-sensitive mMRI nanosensor can be used for measuring the endogenous release of acetylcholine in the rat brain after its intracerebral administration [294]. Similarly, after intracerebral administration of alginate-coated IONPs, changes in Ca^{2+} levels have been monitored following a quinolinic acid-induced striatal lesion [295]. Other magnetic nanostructures have been used for the detection of brain inflammation [296]. These particular nanostructures are based on IONPs coupled covalently through peptide linkers that have been designed to be cleaved by the intracellular macrophage cathepsin, which results in microparticles of iron oxide (MPIO) and allows the fate of magnetic NPs to be tracked. This is because the MPIO, once sequestered by macrophages in the liver, decrease their relaxivity, while particles that associate with their target tissue in the brain remain unaltered and functional.

Thrombosis is a major clinical problem whose incidence has not decreased over the last 20 years and is involved in several pathological disorders such as myocardial infarction, ischemic stroke or pulmonary embolism, among others [297]. Early detection is essential for effective treatment, but it remains challenging in practice. P-selectin is an adhesion molecule, overexpressed at the surface of endothelial cells and platelets upon activation, which plays a fundamental role in thrombus formation [298]. Based on this fact, Suzuki et al. [299] innovated a fucoidan (a natural sulfated polysaccharide with high affinity for activated platelets through P-selectin)-coated USPIONs to visualize by MRI arterial thrombi in the early stage of the disease. Other investigations used PLGA-coated IONs, functionalized with EWVDV peptide, which has a high affinity and specificity for P-selectin, to target thrombi for both diagnosis and treatment through the induction of thrombolysis [300].

4.3 Other Applications

IONPs have also been used in combination with MRI for many other in vivo applications, such as imaging of activated microglia during brain inflammation [301], tracking of stem cells [302–304], image-guided treatment of anemia using bacteria loaded with IONPs [305], or to carry out vascular imaging [306, 307], among others.

5 Conclusions

Recent advances in nanotechnology applied to biomedical research have made possible the development of a new generation of magnetic nanomaterials with great potential as MRI CAs. IONPs stand out due to their excellent combination of properties for in vivo applications, that is, their superparamagnetism along with their high biocompatibility. Also, advanced functionalization strategies have allowed these IONPs to be specifically targeted to different tissues or cells to perform molecular imaging. However, in spite of all these advances, and the large number of studies carried out in this field, very little clinical translation has been achieved so far. The main reasons behind this relative failure are very likely related to reproducibility and scalability issues during the synthesis process, which must be further improved. Also, in vivo studies must be thoroughly designed to include comprehensive toxicity assays and preclinical imaging studies using appropriate animal models.

Acknowledgements Ashish Avasthi thanks the Marie Curie COFUND program for her PhD scholarship (NanoMedPhD, Grant agreement 713721). Financial support was provided by the Spanish Ministry of Science, Innovation and Universities (CTQ2017-86655-R) to María Luisa García-Martín and Manuel Pernia Leal. Manuel Pernia Leal also thanks the "V Plan Propio" of the University of Seville for his Postdoctoral Fellowship.

References

1. García-Martín ML, López-Larrubia P (2018) Preclinical MRI: methods and protocols, vol 1718. Methods in molecular biology. Springer, New York
2. Xie W, Guo Z, Gao F, Gao Q, Wang D, Liaw B-s, Cai Q, Sun X, Wang X, Zhao L (2018) Shape-, size- and structure-controlled synthesis and biocompatibility of iron oxide nanoparticles for magnetic theranostics. Theranostics 8(12):3284–3307. https://doi.org/10.7150/thno.25220
3. Leong HS, Butler KS, Brinker CJ, Azzawi M, Conlan S, Dufés C, Owen A, Rannard S, Scott C, Chen C, Dobrovolskaia MA, Kozlov SV, Prina-Mello A, Schmid R, Wick P, Caputo F, Boisseau P, Crist RM, McNeil SE, Fadeel B, Tran L, Hansen SF, Hartmann NB, Clausen LPW, Skjolding LM, Baun A, Ågerstrand M, Gu Z, Lamprou DA, Hoskins C, Huang L, Song W, Cao H, Liu X, Jandt KD, Jiang W, Kim BYS, Wheeler KE, Chetwynd AJ, Lynch I, Moghimi SM, Nel A, Xia T, Weiss PS, Sarmento B, das Neves J, Santos HA, Santos L, Mitragotri S, Little S, Peer D, Amiji MM, Alonso MJ, Petri-Fink A, Balog S, Lee A, Drasler B, Rothen-Rutishauser B, Wilhelm S, Acar H, Harrison RG, Mao C, Mukherjee P, Ramesh R, McNally LR, Busatto S, Wolfram J, Bergese P, Ferrari M, Fang RH, Zhang L, Zheng J, Peng C, Du B, Yu M, Charron DM, Zheng G, Pastore C (2019) On the issue of transparency and reproducibility in nanomedicine. Nat Nanotechnol 14(7):629–635. https://doi.org/10.1038/s41565-019-0496-9

4. Wu W, He Q, Jiang C (2008) Magnetic iron oxide nanoparticles: synthesis and surface functionalization strategies. Nanosc Res Lett 3(11):397–415. https://doi.org/10.1007/s11671-008-9174-9
5. Zhi D, Yang T, Yang J, Fu S, Zhang S (2020) Targeting strategies for superparamagnetic iron oxide nanoparticles in cancer therapy. Acta Biomater 102:13–34. https://doi.org/10.1016/j.actbio.2019.11.027
6. Ventola CL (2017) Progress in nanomedicine: approved and investigational nanodrugs. Pharm Therap 42(12):742–755
7. Massart R (1981) Preparation of aqueous magnetic liquids in alkaline and acidic media. IEEE Trans Magn 17(2):1247–1248. https://doi.org/10.1109/TMAG.1981.1061188
8. Le Fort J (1852) C R Acad Sci Paris 34:480
9. Elmore WC (1938) The magnetization of ferromagnetic colloids. Phys Rev 54(12):1092–1095. https://doi.org/10.1103/PhysRev.54.1092
10. LaMer VK, Dinegar RH (1950) Theory, production and mechanism of formation of monodispersed hydrosols. J Am Chem Soc 72(11):4847–4854. https://doi.org/10.1021/ja01167a001
11. Banfield JF, Welch SA, Zhang H, Ebert TT, Penn RL (2000) Aggregation-based crystal growth and microstructure development in natural iron oxyhydroxide biomineralization products. Science 289(5480):751–754. https://doi.org/10.1126/science.289.5480.751
12. Boistelle R, Astier JP (1988) Crystallization mechanisms in solution. J Cryst Growth 90(1):14–30. https://doi.org/10.1016/0022-0248(88)90294-1
13. Penn RL, Banfield JF (1998) Imperfect oriented attachment: dislocation generation in defect-free nanocrystals. Science 281(5379):969–971. https://doi.org/10.1126/science.281.5379.969
14. Penn RL, Banfield JF (1999) Morphology development and crystal growth in nanocrystalline aggregates under hydrothermal conditions: insights from titania. Geochim Cosmochim Acta 63(10):1549–1557. https://doi.org/10.1016/S0016-7037(99)00037-X
15. LaGrow AP, Besenhard MO, Hodzic A, Sergides A, Bogart LK, Gavriilidis A, Thanh NTK (2019) Unravelling the growth mechanism of the co-precipitation of iron oxide nanoparticles with the aid of synchrotron X-ray diffraction in solution. Nanoscale 11(14):6620–6628. https://doi.org/10.1039/c9nr00531e
16. Bee A, Massart R, Neveu S (1995) Synthesis of very fine maghemite particles. J Magn Magn Mater 149(1):6–9. https://doi.org/10.1016/0304-8853(95)00317-7
17. Babes L, Denizot B, Tanguy G, Le Jeune JJ, Jallet P (1999) Synthesis of iron oxide nanoparticles used as MRI contrast agents: a parametric study. J Colloid Interface Sci 212(2):474–482. https://doi.org/10.1006/jcis.1998.6053
18. Qiu X-P (2000) Synthesis and characterization of magnetic nano particles. Chin J Chem 18(6):834–837. https://doi.org/10.1002/cjoc.20000180607
19. da Costa GM, De Grave E, de Bakker PMA, Vandenberghe RE (1994) Synthesis and characterization of some iron oxides by sol–gel method. J Solid State Chem 113(2):405–412. https://doi.org/10.1006/jssc.1994.1388
20. Sjogren CE, Briley-Saebo K, Hanson M, Johansson C (1994) Magnetic characterization of iron oxides for magnetic resonance imaging. Magn Reson Med 31(3):268–272. https://doi.org/10.1002/mrm.1910310305
21. Gupta AK, Curtis AS (2004) Lactoferrin and ceruloplasmin derivatized superparamagnetic iron oxide nanoparticles for targeting cell surface receptors. Biomaterials 25(15):3029–3040. https://doi.org/10.1016/j.biomaterials.2003.09.095
22. Kim DK, Zhang Y, Voit W, Rao KV, Muhammed M (2001) Synthesis and characterization of surfactant-coated superparamagnetic monodispersed iron oxide nanoparticles. J Magn Magn Mater 225(1):30–36. https://doi.org/10.1016/S0304-8853(00)01224-5
23. Vayssières L, Chanéac C, Tronc E, Jolivet JP (1998) Size tailoring of magnetite particles formed by aqueous precipitation: an example of thermodynamic stability of nanometric oxide particles. J Colloid Interface Sci 205(2):205–212. https://doi.org/10.1006/jcis.1998.5614
24. Jiang W, Yang HC, Yang SY, Horng HE, Hung JC, Chen YC, Hong C-Y (2004) Preparation and properties of superparamagnetic nanoparticles with narrow size distribution and biocompatible. J Magn Magn Mater 283(2):210–214. https://doi.org/10.1016/j.jmmm.2004.05.022
25. Tominaga M, Matsumoto M, Soejima K, Taniguchi I (2006) Size control for two-dimensional iron oxide nanodots derived from biological molecules. J Colloid Interface Sci 299(2):761–765. https://doi.org/10.1016/j.jcis.2006.02.022

26. Itoh H, Sugimoto T (2003) Systematic control of size, shape, structure, and magnetic properties of uniform magnetite and maghemite particles. J Colloid Interface Sci 265(2):283–295. https://doi.org/10.1016/S0021-9797(03)00511-3
27. Pardoe H, Chua-anusorn W, St. PierreDobson TGJ (2001) Structural and magnetic properties of nanoscale iron oxide particles synthesized in the presence of dextran or polyvinyl alcohol. J Magn Magn Mater 225(1):41–46. https://doi.org/10.1016/S0304-8853(00)01226-9
28. Thapa D, Palkar VR, Kurup MB, Malik SK (2004) Properties of magnetite nanoparticles synthesized through a novel chemical route. Mater Lett 58(21):2692–2694. https://doi.org/10.1016/j.matlet.2004.03.045
29. Khalafalla S, Reimers G (1980) Preparation of dilution-stable aqueous magnetic fluids. IEEE Trans Magn 16(2):178–183. https://doi.org/10.1109/TMAG.1980.1060578
30. Jolivet J-P, Froidefond C, Pottier A, Chanéac C, Cassaignon S, Tronc E, Euzen P (2004) Size tailoring of oxide nanoparticles by precipitation in aqueous medium. A semi-quantitative modelling. J Mater Chem 14(21):3281–3288. https://doi.org/10.1039/B407086K
31. Bui TQ, Ton SN-C, Duong AT, Tran HT (2018) Size-dependent magnetic responsiveness of magnetite nanoparticles synthesised by co-precipitation and solvothermal methods. J Sci Adv Mater Devices 3(1):107–112. https://doi.org/10.1016/j.jsamd.2017.11.002
32. Thomas JR (1966) Preparation and magnetic properties of colloidal cobalt particles. J Appl Phys 37(7):2914–2915. https://doi.org/10.1063/1.1782154
33. Smith TW, Wychick D (1980) Colloidal iron dispersions prepared via the polymer-catalyzed decomposition of iron pentacarbonyl. J Phys Chem 84:1621–1629. https://doi.org/10.1021/j100449a037
34. Hess PH, Parker PH Jr (1966) Polymers for stabilization of colloidal cobalt particles. J Appl Polym Sci 10(12):1915–1927. https://doi.org/10.1002/app.1966.070101209
35. Peter K, Vollhardt C, Bercaw JE, Bergman RG (1975) Photochemistry of η5 cylclopentadienylcobalt) tricarbonyl, tris(η5-cyclopentadienylcobalt monocarbonyl) and tetra(η5-cyclopentadienylcobalt) dicarbonyl*. J Organomet Chem 97(2):283–297. https://doi.org/10.1016/S0022-328X(00)89475-9
36. Van Wonterghem J, Mørup S, Charles SW, Wells S (1988) An investigation of the chemical reactions leading to the formation of ultrafine amorphous fe100−xcx alloy particles. J Colloid Interface Sci 121(2):558–563. https://doi.org/10.1016/0021-9797(88)90457-2
37. Hyeon T, Lee SS, Park J, Chung Y, Na HB (2001) Synthesis of highly crystalline and monodisperse maghemite nanocrystallites without a size-selection process. J Am Chem Soc 123(51):12798–12801. https://doi.org/10.1021/ja016812s
38. Jana NR, Chen Y, Peng X (2004) Size- and shape-controlled magnetic (Cr, Mn, Fe Co, Ni) oxide nanocrystals via a simple and general approach. Chem Mater 16(20):3931–3935. https://doi.org/10.1021/cm049221k
39. Lassenberger A, Grünewald TA, van Oostrum PDJ, Rennhofer H, Amenitsch H, Zirbs R, Lichtenegger HC, Reimhult E (2017) Monodisperse iron oxide nanoparticles by thermal decomposition: elucidating particle formation by second-resolved in situ small-angle X-ray scattering. Chem Mater 29(10):4511–4522. https://doi.org/10.1021/acs.chemmater.7b01207
40. Kwon SG, Piao Y, Park J, Angappane S, Jo Y, Hwang NM, Park JG, Hyeon T (2007) Kinetics of monodisperse iron oxide nanocrystal formation by "heating-up" process. J Am Chem Soc 129(41):12571–12584. https://doi.org/10.1021/ja074633q
41. Kim BH, Shin K, Kwon SG, Jang Y, Lee H-S, Lee H, Jun SW, Lee J, Han SY, Yim Y-H, Kim D-H, Hyeon T (2013) Sizing by weighing: characterizing sizes of ultrasmall-sized iron oxide nanocrystals using MALDI-TOF mass spectrometry. J Am Chem Soc 135(7):2407–2410. https://doi.org/10.1021/ja310030c
42. Kura H, Takahashi M, Ogawa T (2010) Synthesis of monodisperse iron nanoparticles with a high saturation magnetization using an Fe(CO)x−oleylamine reacted precursor. J Phys Chem C 114(13):5835–5838. https://doi.org/10.1021/jp911161g
43. Sun S, Zeng H, Robinson DB, Raoux S, Rice PM, Wang SX, Li G (2004) Monodisperse MFe_2O_4 (M = Fe Co, Mn) nanoparticles. J Am Chem Soc 126(1):273–279. https://doi.org/10.1021/ja038 0852
44. Rockenberger J, Scher EC, Alivisatos AP (1999) A new nonhydrolytic single-precursor approach to surfactant-capped nanocrystals of transition metal oxides. J Am Chem Soc 121(49):11595–11596. https://doi.org/10.1021/ja993280v

45. Park J, An K, Hwang Y, Park JG, Noh HJ, Kim JY, Park JH, Hwang NM, Hyeon T (2004) Ultra-large-scale syntheses of monodisperse nanocrystals. Nat Mater 3(12):891–895. https://doi.org/10.1038/nmat1251
46. Park S-J, Kim S, Lee S, Khim ZG, Char K, Hyeon T (2000) Synthesis and magnetic studies of uniform iron nanorods and nanospheres. J Am Chem Soc 122(35):8581–8582. https://doi.org/10.1021/ja001628c
47. Zhang H, Li L, Liu XL, Jiao J, Ng C-T, Yi JB, Luo YE, Bay B-H, Zhao LY, Peng ML, Gu N, Fan HM (2017) Ultrasmall ferrite nanoparticles synthesized via dynamic simultaneous thermal decomposition for high-performance and multifunctional T1 magnetic resonance imaging contrast agent. ACS Nano 11(4):3614–3631. https://doi.org/10.1021/acsnano.6b07684
48. Roca AG, Morales MP, Serna CJ (2006) Synthesis of monodispersed magnetite particles from different organometallic precursors. IEEE Trans Magn 42(10):3025–3029. https://doi.org/10.1109/TMAG.2006.880111
49. Guardia P, Riedinger A, Nitti S, Pugliese G, Marras S, Genovese A, Materia ME, Lefevre C, Manna L, Pellegrino T (2014) One pot synthesis of monodisperse water soluble iron oxide nanocrystals with high values of the specific absorption rate. J Mater Chem B 2(28):4426–4434. https://doi.org/10.1039/C4TB00061G
50. Kim BH, Lee N, Kim H, An K, Park YI, Choi Y, Shin K, Lee Y, Kwon SG, Na HB, Park J-G, Ahn T-Y, Kim Y-W, Moon WK, Choi SH, Hyeon T (2011) Large-scale synthesis of uniform and extremely small-sized iron oxide nanoparticles for high-resolution T1 magnetic resonance imaging contrast agents. J Am Chem Soc 133(32):12624–12631. https://doi.org/10.1021/ja203340u
51. Kovalenko MV, Bodnarchuk MI, Lechner RT, Hesser G, Schäffler F, Heiss W (2007) Fatty acid salts as stabilizers in size- and shape-controlled nanocrystal synthesis: the case of inverse spinel iron oxide. J Am Chem Soc 129(20):6352–6353. https://doi.org/10.1021/ja0692478
52. Mourdikoudis S, Liz-Marzán LM (2013) Oleylamine in nanoparticle synthesis. Chem Mater 25(9):1465–1476. https://doi.org/10.1021/cm4000476
53. Hou Y, Xu Z, Sun S (2007) Controlled synthesis and chemical conversions of FeO nanoparticles. Angew Chem Int Ed 46(33):6329–6332. https://doi.org/10.1002/anie.200701694
54. Nemati Z, Alonso J, Rodrigo I, Das R, Garaio E, García JÁ, Orue I, Phan M-H, Srikanth H (2018) Improving the heating efficiency of iron oxide nanoparticles by tuning their shape and size. J Phys Chem C 122(4):2367–2381. https://doi.org/10.1021/acs.jpcc.7b10528
55. Park J, Lee E, Hwang N-M, Kang M, Kim SC, Hwang Y, Park J-G, Noh H-J, Kim J-Y, Park J-H, Hyeon T (2005) One-nanometer-scale size-controlled synthesis of monodisperse magnetic iron oxide nanoparticles. Angew Chem Int Ed 44(19):2872–2877. https://doi.org/10.1002/anie.200461665
56. Li Z, Sun Q, Gao M (2005) Preparation of water-soluble magnetite nanocrystals from hydrated ferric salts in 2-pyrrolidone: mechanism leading to Fe_3O_4. Angew Chem Int Ed 44(1):123–126. https://doi.org/10.1002/anie.200460715
57. Xu Z, Shen C, Hou Y, Gao H, Sun S (2009) Oleylamine as both reducing agent and stabilizer in a facile synthesis of magnetite nanoparticles. Chem Mater 21(9):1778–1780. https://doi.org/10.1021/cm802978z
58. Yang H, Ogawa T, Hasegawa D, Takahashi M (2008) Synthesis and magnetic properties of monodisperse magnetite nanocubes. J Appl Phys 103(7):07D526. https://doi.org/10.1063/1.2833820
59. Mohapatra J, Mitra A, Bahadur D, Aslam M (2013) Surface controlled synthesis of MFe_2O_4 (M = Mn, Fe Co, Ni and Zn) nanoparticles and their magnetic characteristics. CrystEngComm 15(3):524–532. https://doi.org/10.1039/C2CE25957E
60. Macdonald JE, Brooks CJ, Veinot JGC (2008) The influence of trace water concentration on iron oxide nanoparticle size. Chem Commun 32:3777–3779. https://doi.org/10.1039/B805715J
61. Unni M, Uhl AM, Savliwala S, Savitzky BH, Dhavalikar R, Garraud N, Arnold DP, Kourkoutis LF, Andrew JS, Rinaldi C (2017) Thermal decomposition synthesis of iron oxide nanoparticles with diminished magnetic dead layer by controlled addition of oxygen. ACS Nano 11(2):2284–2303. https://doi.org/10.1021/acsnano.7b00609
62. Li Z, Chen H, Bao H, Gao M (2004) One-pot reaction to synthesize water-soluble magnetite nanocrystals. Chem Mater 16(8):1391–1393. https://doi.org/10.1021/cm035346y
63. Ooi F, DuChene JS, Qiu J, Graham JO, Engelhard MH, Cao G, Gai Z, Wei WD (2015) A facile solvothermal synthesis of octahedral Fe_3O_4 nanoparticles. Small 11(22):2649–2653. https://doi.org/10.1002/smll.201401954

64. Bunge A, Porav AS, Borodi G, Radu T, Pîrnău A, Berghian-Grosan C, Turcu R (2019) Correlation between synthesis parameters and properties of magnetite clusters prepared by solvothermal polyol method. J Mater Sci 54(4):2853–2875. https://doi.org/10.1007/s10853-018-3030-9
65. Mao B, Kang Z, Wang E, Lian S, Gao L, Tian C, Wang C (2006) Synthesis of magnetite octahedrons from iron powders through a mild hydrothermal method. Mater Res Bull 41(12):2226–2231. https://doi.org/10.1016/j.materresbull.2006.04.037
66. Giri J, Guha Thakurta S, Bellare J, Kumar Nigam A, Bahadur D (2005) Preparation and characterization of phospholipid stabilized uniform sized magnetite nanoparticles. J Magn Magn Mater 293(1):62–68. https://doi.org/10.1016/j.jmmm.2005.01.044
67. Wang J, Sun J, Sun Q, Chen Q (2003) One-step hydrothermal process to prepare highly crystalline Fe_3O_4 nanoparticles with improved magnetic properties. Mater Res Bull 38(7):1113–1118. https://doi.org/10.1016/S0025-5408(03)00129-6
68. Li J, Shi X, Shen M (2014) Hydrothermal synthesis and functionalization of iron oxide nanoparticles for mr imaging applications. Part Part Syst Charact 31(12):1223–1237. https://doi.org/10.1002/ppsc.201400087
69. Lassoued A, Lassoued MS, Dkhil B, Ammar S, Gadri A (2018) Synthesis, photoluminescence and magnetic properties of iron oxide (α-Fe_2O_3) nanoparticles through precipitation or hydrothermal methods. Phys E 101:212–219. https://doi.org/10.1016/j.physe.2018.04.009
70. Pinna N, Grancharov S, Beato P, Bonville P, Antonietti M, Niederberger M (2005) Magnetite nanocrystals: nonaqueous synthesis, characterization, and solubility. Chem Mater 17(11):3044–3049. https://doi.org/10.1021/cm050060+
71. Nassar MY, Ahmed IS, Hendy HS (2018) A facile one-pot hydrothermal synthesis of hematite (α-Fe_2O_3) nanostructures and cephalexin antibiotic sorptive removal from polluted aqueous media. J Mol Liq 271:844–856. https://doi.org/10.1016/j.molliq.2018.09.057
72. Wilson D, Langell MA (2014) XPS analysis of oleylamine/oleic acid capped Fe_3O_4 nanoparticles as a function of temperature. Appl Surf Sci 303:6–13. https://doi.org/10.1016/j.apsusc.2014.02.006
73. Brewster DA, Sarappa DJ, Knowles KE (2019) Role of aliphatic ligands and solvent composition in the solvothermal synthesis of iron oxide nanocrystals. Polyhedron 157:54–62. https://doi.org/10.1016/j.poly.2018.09.063
74. Huang J, Han J, Wang R, Zhang Y, Wang X, Zhang X, Zhang Z, Zhang Y, Song B, Jin S (2018) Improving electrocatalysts for oxygen evolution using $Ni_xFe_{3-x}O_4$/Ni hybrid nanostructures formed by solvothermal synthesis. ACS Energy Lett 3(7):1698–1707. https://doi.org/10.1021/acsenergylett.8b00888
75. Kim J, Tran VT, Oh S, Kim C-S, Hong JC, Kim S, Joo Y-S, Mun S, Kim M-H, Jung J-W, Lee J, Kang YS, Koo J-W, Lee J (2018) Scalable solvothermal synthesis of superparamagnetic Fe_3O_4 nanoclusters for bioseparation and theragnostic probes. ACS Appl Mater Interfaces 10(49):41935–41946. https://doi.org/10.1021/acsami.8b14156
76. Xiao J, Zhang G, Qian J, Sun X, Tian J, Zhong K, Cai D, Wu Z (2018) Fabricating high-performance T2-weighted contrast agents via adjusting composition and size of nanomagnetic iron oxide. ACS Appl Mater Interfaces 10(8):7003–7011. https://doi.org/10.1021/acsami.8b00428
77. Köçkar H, Karaagac O, Özel F (2019) Effects of biocompatible surfactants on structural and corresponding magnetic properties of iron oxide nanoparticles coated by hydrothermal process. J Magn Magn Mater 474:332–336. https://doi.org/10.1016/j.jmmm.2018.11.053
78. Fievet F, Lagier JP, Blin B, Beaudoin B, Figlarz M (1989) Homogeneous and heterogeneous nucleations in the polyol process for the preparation of micron and submicron size metal particles. Solid State Ion 32–33:198–205. https://doi.org/10.1016/0167-2738(89)90222-1
79. Viau G, Fiévet-Vincent F, Fiévet F, Toneguzzo P, Ravel F, Acher O (1997) Size dependence of microwave permeability of spherical ferromagnetic particles. J Appl Phys 81(6):2749–2754. https://doi.org/10.1063/1.363979
80. Chakroune N, Viau G, Ricolleau C, Fiévet-Vincent F, Fiévet F (2003) Cobalt-based anisotropic particles prepared by the polyol process. J Mater Chem 13(2):312–318. https://doi.org/10.1039/B209383A
81. Viau G, Toneguzzo P, Pierrard A, Acher O, Fiévet-Vincent F, Fiévet F (2001) Heterogeneous nucleation and growth of metal nanoparticles in polyols. Script Mater 44(8):2263–2267. https://doi.org/10.1016/S1359-6462(01)00752-7
82. Ammar S, Helfen A, Jouini N, Fiévet F, Rosenman I, Villain F, Molinié P, Danot M (2001) Magnetic properties of ultrafine cobalt ferrite particles synthesized by hydrolysis in a polyol medium. J Mater Chem 11(1):186–192. https://doi.org/10.1039/B003193N

83. Chow GM, Kurihara LK, Kemner KM, Schoen PE, Elam WT, Ervin A, Keller S, Zhang YD, Budnick J, Ambrose T (2011) Structural, morphological, and magnetic study of nanocrystalline cobalt-copper powders synthesized by the polyol process. J Mater Res 10(6):1546–1554. https://doi.org/10.1557/JMR.1995.1546
84. Jungk HO, Feldmann C (2011) Nonagglomerated, submicron α-Fe_2O_3 particles: preparation and application. J Mater Res 15(10):2244–2248. https://doi.org/10.1557/JMR.2000.0322
85. Caruntu D, Caruntu G, Chen Y, O'Connor CJ, Goloverda G, Kolesnichenko VL (2004) Synthesis of variable-sized nanocrystals of Fe_3O_4 with high surface reactivity. Chem Mater 16(25):5527–5534. https://doi.org/10.1021/cm0487977
86. Joseyphus RJ, Kodama D, Matsumoto T, Sato Y, Jeyadevan B, Tohji K (2007) Role of polyol in the synthesis of Fe particles. J Magn Magn Mater 310(2 Part 3):2393–2395. https://doi.org/10.1016/j.jmmm.2006.10.1132
87. Cheng C, Xu F, Gu H (2011) Facile synthesis and morphology evolution of magnetic iron oxide nanoparticles in different polyol processes. New J Chem 35(5):1072–1079. https://doi.org/10.1039/C0NJ00986E
88. Hachani R, Lowdell M, Birchall M, Hervault A, Mertz D, Begin-Colin S, Thanh NTK (2016) Polyol synthesis, functionalisation, and biocompatibility studies of superparamagnetic iron oxide nanoparticles as potential MRI contrast agents. Nanoscale 8(6):3278–3287. https://doi.org/10.1039/C5NR03867G
89. Gavilán H, Sánchez EH, Brollo MEF, Asín L, Moerner KK, Frandsen C, Lázaro FJ, Serna CJ, Veintemillas-Verdaguer S, Morales MP, Gutiérrez L (2017) Formation mechanism of maghemite nanoflowers synthesized by a polyol-mediated process. ACS Omega 2(10):7172–7184. https://doi.org/10.1021/acsomega.7b00975
90. Hu F, MacRenaris KW, Waters EA, Liang T, Schultz-Sikma EA, Eckermann AL, Meade TJ (2009) Ultrasmall, water-soluble magnetite nanoparticles with high relaxivity for magnetic resonance imaging. J Phys Chem C 113(49):20855–20860. https://doi.org/10.1021/jp907216g
91. Wan J, Cai W, Meng X, Liu E (2007) Monodisperse water-soluble magnetite nanoparticles prepared by polyol process for high-performance magnetic resonance imaging. Chem Commun 47:5004–5006. https://doi.org/10.1039/B712795B
92. Cai W, Wan J (2007) Facile synthesis of superparamagnetic magnetite nanoparticles in liquid polyols. J Colloid Interface Sci 305(2):366–370. https://doi.org/10.1016/j.jcis.2006.10.023
93. Hemery G, Keyes AC, Garaio E, Rodrigo I, Garcia JA, Plazaola F, Garanger E, Sandre O (2017) Tuning sizes, morphologies, and magnetic properties of monocore versus multicore iron oxide nanoparticles through the controlled addition of water in the polyol synthesis. Inorg Chem 56(14):8232–8243. https://doi.org/10.1021/acs.inorgchem.7b00956
94. Wetegrove M, Witte K, Bodnar W, Pfahl D-E, Springer A, Schell N, Westphal F, Burkel E (2019) Formation of maghemite nanostructures in polyol: tuning the particle size via the precursor stoichiometry. CrystEngComm 21(12):1956–1966. https://doi.org/10.1039/C8CE02115E
95. Maity D, Chandrasekharan P, Si-Shen F, Xue J-M, Ding J (2010) Polyol-based synthesis of hydrophilic magnetite nanoparticles. J Appl Phys 107(9):09B310. https://doi.org/10.1063/1.3355898
96. Qu H, Ma H, Riviere A, Zhou W, O'Connor CJ (2012) One-pot synthesis in polyamines for preparation of water-soluble magnetite nanoparticles with amine surface reactivity. J Mater Chem 22(8):3311–3313. https://doi.org/10.1039/C2JM15932E
97. Wang J, Zhang B, Wang L, Wang M, Gao F (2015) One-pot synthesis of water-soluble superparamagnetic iron oxide nanoparticles and their MRI contrast effects in the mouse brains. Mater Sci Eng, C 48:416–423. https://doi.org/10.1016/j.msec.2014.12.026
98. Kandasamy G, Soni S, Sushmita K, Veerapu NS, Bose S, Maity D (2019) One-step synthesis of hydrophilic functionalized and cytocompatible superparamagnetic iron oxide nanoparticles (SPIONs) based aqueous ferrofluids for biomedical applications. J Mol Liq 274:653–663. https://doi.org/10.1016/j.molliq.2018.10.161
99. Miao C, Hu F, Rui Y, Duan Y, Gu H (2019) A T1/T2 dual functional iron oxide MRI contrast agent with super stability and low hypersensitivity benefited by ultrahigh carboxyl group density. J Mater Chem B 7(12):2081–2091. https://doi.org/10.1039/C9TB00002J
100. Babić-Stojić B, Jokanović V, Milivojević D, Požek M, Jagličić Z, Makovec D, Orsini NJ, Marković M, Arsikin K, Paunović V (2018) Ultrasmall iron oxide nanoparticles: magnetic and NMR relaxometric properties. Curr Appl Phys 18(2):141–149. https://doi.org/10.1016/j.cap.2017.11.017

101. Yoo D, Lee C, Seo B, Piao Y (2017) One pot synthesis of amine-functionalized and angular-shaped superparamagnetic iron oxide nanoparticles for MR/fluorescence bimodal imaging application. RSC Adv 7(21):12876–12885. https://doi.org/10.1039/C6RA28495G
102. Wagle DV, Rondinone AJ, Woodward JD, Baker GA (2017) Polyol synthesis of magnetite nanocrystals in a thermostable ionic liquid. Cryst Growth Des 17(4):1558–1567. https://doi.org/10.1021/acs.cgd.6b01511
103. Durães L, Costa BFO, Vasques J, Campos J, Portugal A (2005) Phase investigation of as-prepared iron oxide/hydroxide produced by sol–gel synthesis. Mater Lett 59(7):859–863. https://doi.org/10.1016/j.matlet.2004.10.066
104. Masthoff IC, Kraken M, Menzel D, Litterst FJ, Garnweitner G (2016) Study of the growth of hydrophilic iron oxide nanoparticles obtained via the non-aqueous sol–gel method. J Sol-Gel Sci Technol 77(3):553–564. https://doi.org/10.1007/s10971-015-3883-1
105. Venturini J, Wermuth TB, Machado MC, Arcaro S, Alves AK, da Cas VA, Bergmann CP (2019) The influence of solvent composition in the sol–gel synthesis of cobalt ferrite ($CoFe_2O_4$): a route to tuning its magnetic and mechanical properties. J Eur Ceram Soc 39(12):3442–3449. https://doi.org/10.1016/j.jeurceramsoc.2019.01.030
106. Liu XQ, Tao SW, Shen YS (1997) Preparation and characterization of nanocrystalline α-Fe_2O_3 by a sol–gel process. Sens Actuators B Chem 40(2):161–165. https://doi.org/10.1016/S0925-4005(97)80256-0
107. Akbar A, Yousaf H, Riaz S, Naseem S (2019) Role of precursor to solvent ratio in tuning the magnetization of iron oxide thin films—a sol–gel approach. J Magn Magn Mater 471:14–24. https://doi.org/10.1016/j.jmmm.2018.09.008
108. Ba-Abbad MM, Takriff MS, Benamor A, Mohammad AW (2017) Size and shape controlled of α-Fe_2O_3 nanoparticles prepared via sol–gel technique and their photocatalytic activity. J Sol-Gel Sci Technol 81(3):880–893. https://doi.org/10.1007/s10971-016-4228-4
109. Hu P, Chang T, Chen W-J, Deng J, Li S-L, Zuo Y-G, Kang L, Yang F, Hostetter M, Volinsky AA (2019) Temperature effects on magnetic properties of Fe_3O_4 nanoparticles synthesized by the sol–gel explosion-assisted method. J Alloy Compd 773:605–611. https://doi.org/10.1016/j.jallcom.2018.09.238
110. Danks AE, Hall SR, Schnepp Z (2016) The evolution of 'sol–gel' chemistry as a technique for materials synthesis. Mater Horizons 3(2):91–112. https://doi.org/10.1039/C5MH00260E
111. Akbar A, Riaz S, Ashraf R, Naseem S (2015) Magnetic and magnetization properties of iron oxide thin films by microwave assisted sol–gel route. J Sol-Gel Sci Technol 74(2):320–328. https://doi.org/10.1007/s10971-014-3528-9
112. Kopanja L, Milosevic I, Panjan M, Damnjanovic V, Tadic M (2016) Sol–gel combustion synthesis, particle shape analysis and magnetic properties of hematite (α-Fe_2O_3) nanoparticles embedded in an amorphous silica matrix. Appl Surf Sci 362:380–386. https://doi.org/10.1016/j.apsusc.2015.11.238
113. Kralj S, Makovec D (2015) Magnetic assembly of superparamagnetic iron oxide nanoparticle clusters into nanochains and nanobundles. ACS Nano 9(10):9700–9707. https://doi.org/10.1021/acsnano.5b02328
114. Bagwe RP, Kanicky JR, Palla BJ, Patanjali PK, Shah DO (2001) Improved drug delivery using microemulsions: rationale, recent progress, and new horizons. Crit Rev Ther Drug Carrier Syst 18(1):77–140
115. Okoli C, Sanchez-Dominguez M, Boutonnet M, Jaras S, Civera C, Solans C, Kuttuva GR (2012) Comparison and functionalization study of microemulsion-prepared magnetic iron oxide nanoparticles. Langmuir 28(22):8479–8485. https://doi.org/10.1021/la300599q
116. Inouye K, Endo R, Otsuka Y, Miyashiro K, Kaneko K, Ishikawa T (1982) Oxygenation of ferrous ions in reversed micelle and reversed microemulsion. J Phys Chem 86(8):1465–1469. https://doi.org/10.1021/j100397a051
117. Lawrence MJ (1994) Surfactant systems: microemulsions and vesicles as vehicles for drug delivery. Eur J Drug Metab Pharmacokinet 19(3):257–269. https://doi.org/10.1007/BF03188929
118. Lawrence MJ, Rees GD (2000) Microemulsion-based media as novel drug delivery systems. Adv Drug Deliv Rev 45(1):89–121. https://doi.org/10.1016/S0169-409X(00)00103-4
119. Fendler JH (1987) Atomic and molecular clusters in membrane mimetic chemistry. Chem Rev 87(5):877–899. https://doi.org/10.1021/cr00081a002

120. Munshi N, De TK, Maitra A (1997) Size modulation of polymeric nanoparticles under controlled dynamics of microemulsion droplets. J Colloid Interface Sci 190(2):387–391. https://doi.org/10.1006/jcis.1997.4889
121. Gupta AK, Wells S (2004) Surface-modified superparamagnetic nanoparticles for drug delivery: preparation, characterization, and cytotoxicity studies. IEEE Trans Nanobiosci 3(1):66–73. https://doi.org/10.1109/TNB.2003.820277
122. Igartua M, Saulnier P, Heurtault B, Pech B, Proust JE, Pedraz JL, Benoit JP (2002) Development and characterization of solid lipid nanoparticles loaded with magnetite. Int J Pharm 233(1):149–157. https://doi.org/10.1016/S0378-5173(01)00936-X
123. Yaacob II, Nunes AC, Bose A, Shah DO (1994) Synthesis and characterization of magnetic nanoparticles in spontaneously generated vesicles. J Colloid Interface Sci 168(2):289–301. https://doi.org/10.1006/jcis.1994.1423
124. Uchida M, Flenniken ML, Allen M, Willits DA, Crowley BE, Brumfield S, Willis AF, Jackiw L, Jutila M, Young MJ, Douglas T (2006) Targeting of cancer cells with ferrimagnetic ferritin cage nanoparticles. J Am Chem Soc 128(51):16626–16633. https://doi.org/10.1021/ja0655690
125. Bhandarkar S, Bose A (1990) Synthesis of nanocomposite particles by intravesicular coprecipitation. J Colloid Interface Sci 139(2):541–550. https://doi.org/10.1016/0021-9797(90)90127-A
126. Yaacob II, Nunes AC, Bose A (1995) Magnetic nanoparticles produced in spontaneous cationic-anionic vesicles: room temperature synthesis and characterization. J Colloid Interface Sci 171(1):73–84. https://doi.org/10.1006/jcis.1995.1152
127. Najafi A, Nematipour K (2017) Synthesis and magnetic properties evaluation of monosized FeCo alloy nanoparticles through microemulsion method. J Supercond Novel Magn 30(9):2647–2653. https://doi.org/10.1007/s10948-017-4052-2
128. Singh P, Upadhyay C (2018) Fine tuning of size and morphology of magnetite nanoparticles synthesized by microemulsion. AIP Conf Proc 1953 1:030051. https://doi.org/10.1063/1.5032386
129. Bonacchi D, Caneschi A, Dorignac D, Falqui A, Gatteschi D, Rovai D, Sangregorio C, Sessoli R (2004) Nanosized iron oxide particles entrapped in pseudo-single crystals of γ-cyclodextrin. Chem Mater 16(10):2016–2020. https://doi.org/10.1021/cm034948e
130. Lee Y, Lee J, Bae CJ, Park JG, Noh HJ, Park JH, Hyeon T (2005) Large-scale synthesis of uniform and crystalline magnetite nanoparticles using reverse micelles as nanoreactors under reflux conditions. Adv Func Mater 15(3):503–509. https://doi.org/10.1002/adfm.200400187
131. Vidal-Vidal J, Rivas J, López-Quintela MA (2006) Synthesis of monodisperse maghemite nanoparticles by the microemulsion method. Colloids Surf A 288(1):44–51. https://doi.org/10.1016/j.colsurfa.2006.04.027
132. Pileni M-P (2003) The role of soft colloidal templates in controlling the size and shape of inorganic nanocrystals. Nat Mater 2(3):145–150. https://doi.org/10.1038/nmat817
133. Han X, Yao P, Cheng C, Yuan H, Yang Y, Ni C (2018) Preparation and in vivo biodistribution of ultra-small superparamagnetic iron oxide nanoparticles with high magnetic targeting response. J Nanosci Nanotechnol 18(2):879–886. https://doi.org/10.1166/jnn.2018.14110
134. De Cuyper M, Joniau M (1988) Magnetoliposomes. Eur Biophys J 15(5):311–319. https://doi.org/10.1007/BF00256482
135. Rocha FM, de Pinho SC, Zollner RL, Santana MHA (2001) Preparation and characterization of affinity magnetoliposomes useful for the detection of antiphospholipid antibodies. J Magn Magn Mater 225(1):101–108. https://doi.org/10.1016/S0304-8853(00)01236-1
136. Bulte JWM, Cuyper Md, Despres D, Frank JA (1999) Preparation, relaxometry, and biokinetics of PEGylated magnetoliposomes as MR contrast agent. J Magn Magn Mater 194(1):204–209. https://doi.org/10.1016/S0304-8853(98)00556-3
137. Lesieur S, Grabielle-Madelmont C, Ménager C, Cabuil V, Dadhi D, Pierrot P, Edwards K (2003) Evidence of surfactant-induced formation of transient pores in lipid bilayers by using magnetic-fluid-loaded liposomes. J Am Chem Soc 125(18):5266–5267. https://doi.org/10.1021/ja021471j
138. Nobuto H, Sugita T, Kubo T, Shimose S, Yasunaga Y, Murakami T, Ochi M (2004) Evaluation of systemic chemotherapy with magnetic liposomal doxorubicin and a dipole external electromagnet. Int J Cancer 109(4):627–635. https://doi.org/10.1002/ijc.20035
139. Sangregorio C, Wiemann JK, O'Connor CJ, Rosenzweig Z (1999) A new method for the synthesis of magnetoliposomes. J Appl Phys 85(8):5699–5701. https://doi.org/10.1063/1.370256
140. Kaur G, Dogra V, Kumar R, Kumar S, Singh K (2019) Fabrication of iron oxide nanocolloids using metallosurfactant-based microemulsions: antioxidant activity, cellular, and genotoxicity

toward *Vitis vinifera*. J Biomol Struct Dyn 37(4):892–909. https://doi.org/10.1080/07391102.2018.1442251

141. Lee C, Kim GR, Yoon J, Kim SE, Yoo JS, Piao Y (2018) In vivo delineation of glioblastoma by targeting tumor-associated macrophages with near-infrared fluorescent silica coated iron oxide nanoparticles in orthotopic xenografts for surgical guidance. Sci Rep 8(1):11122. https://doi.org/10.1038/s41598-018-29424-4
142. Kampferbeck M, Vossmeyer T, Weller H (2019) Cross-linked polystyrene shells grown on iron oxide nanoparticles via surface-grafted AGET–ATRP in microemulsion. Langmuir 35(26):8790–8798. https://doi.org/10.1021/acs.langmuir.9b01060
143. Cao Y, Min J, Zheng D, Li J, Xue Y, Yu F, Wu M (2019) Vehicle-saving theranostic probes based on hydrophobic iron oxide nanoclusters using doxorubicin as a phase transfer agent for MRI and chemotherapy. Chem Commun 55(61):9015–9018. https://doi.org/10.1039/C9CC03868J
144. Rodríguez-Rodríguez AA, Moreno-Trejo MB, Meléndez-Zaragoza MJ, Collins-Martínez V, López-Ortiz A, Martínez-Guerra E, Sánchez-Domínguez M (2019) Spinel-type ferrite nanoparticles: synthesis by the oil-in-water microemulsion reaction method and photocatalytic water-splitting evaluation. Int J Hydrogen Energy 44(24):12421–12429. https://doi.org/10.1016/j.ijhydene.2018.09.183
145. Amirshaghaghi A, Yan L, Miller J, Daniel Y, Stein JM, Busch TM, Cheng Z, Tsourkas A (2019) Chlorin e6-coated superparamagnetic iron oxide nanoparticle (SPION) nanoclusters as a theranostic agent for dual-mode imaging and photodynamic therapy. Sci Rep 9(1):2613. https://doi.org/10.1038/s41598-019-39036-1
146. Pecharromán C, González-Carreño T, Iglesias JE (1995) The infrared dielectric properties of maghemite, γ-Fe_2O_3, from reflectance measurement on pressed powders. Phys Chem Miner 22(1):21–29. https://doi.org/10.1007/BF00202677
147. González-Carreño T, Morales MP, Gracia M, Serna CJ (1993) Preparation of uniform γ-Fe_2O_3 particles with nanometer size by spray pyrolysis. Mater Lett 18(3):151–155. https://doi.org/10.1016/0167-577X(93)90116-F
148. Che S, Sakurai O, Shinozaki K, Mizutani N (1998) Particle structure control through intraparticle reactions by spray pyrolysis. J Aerosol Sci 29(3):271–278. https://doi.org/10.1016/S0021-8502(97)10012-X
149. Kastrinaki G, Lorentzou S, Karagiannakis G, Rattenbury M, Woodhead J, Konstandopoulos AG (2018) Parametric synthesis study of iron based nanoparticles via aerosol spray pyrolysis route. J Aerosol Sci 115:96–107. https://doi.org/10.1016/j.jaerosci.2017.10.005
150. Zheng J, Liu K, Cai W, Qiao L, Ying Y, Li W, Yu J, Lin M, Che S (2018) Effect of chloride ion on crystalline phase transition of iron oxide produced by ultrasonic spray pyrolysis. Adv Powder Technol 29(9):1953–1959. https://doi.org/10.1016/j.apt.2018.03.028
151. Das H, Debnath N, Toda A, Kawaguchi T, Sakamoto N, Manjura Hoque S, Shinozaki K, Suzuki H, Wakiya N (2018) Controlled synthesis of dense $MgFe_2O_4$ nanospheres by ultrasonic spray pyrolysis technique: effect of ethanol addition to precursor solvent. Adv Powder Technol 29(2):283–288. https://doi.org/10.1016/j.apt.2017.11.014
152. Morales MP, Bomati-Miguel O, Pérez de Alejo R, Ruiz-Cabello J, Veintemillas-Verdaguer S, O'Grady K (2003) Contrast agents for MRI based on iron oxide nanoparticles prepared by laser pyrolysis. J Magn Magn Mater 266(1):102–109. https://doi.org/10.1016/S0304-8853(03)00461-X
153. Miguel OB, Morales MP, Serna CJ, Veintemillas-Verdaguer S (2002) Magnetic nanoparticles prepared by laser pyrolysis. IEEE Trans Magn 38(5):2616–2618. https://doi.org/10.1109/TMAG.2002.801961
154. Zhao XQ, Zheng F, Liang Y, Hu ZQ, Xu YB (1994) Preparation and characterization of single phase γ-Fe nanopowder from cw CO_2 laser induced pyrolysis of iron pentacarbonyl. Mater Lett 21(3):285–288. https://doi.org/10.1016/0167-577X(94)90191-0
155. Julián-López B, Boissière C, Chanéac C, Grosso D, Vasseur S, Miraux S, Duguet E, Sanchez C (2007) Mesoporous maghemite–organosilica microspheres: a promising route towards multifunctional platforms for smart diagnosis and therapy. J Mater Chem 17(16):1563–1569. https://doi.org/10.1039/B615951F
156. Teoh WY, Amal R, Mädler L (2010) Flame spray pyrolysis: an enabling technology for nanoparticles design and fabrication. Nanoscale 2(8):1324–1347. https://doi.org/10.1039/C0NR00017E
157. Mädler L, Kammler HK, Mueller R, Pratsinis SE (2002) Controlled synthesis of nanostructured particles by flame spray pyrolysis. J Aerosol Sci 33(2):369–389. https://doi.org/10.1016/S0021-8502(01)00159-8

158. Xu H, Zeiger BW, Suslick KS (2013) Sonochemical synthesis of nanomaterials. Chem Soc Rev 42(7):2555–2567. https://doi.org/10.1039/C2CS35282F
159. Suslick KS, Nyborg WL (1990) Ultrasound: its chemical, physical and biological effects. J Acoust Soc Am 87(2):919–920. https://doi.org/10.1121/1.398864
160. Suslick KS, Didenko Y, Fang MM, Hyeon T, Kolbeck KJ, McNamara WB, Mdleleni MM, Wong M (1999) Acoustic cavitation and its chemical consequences. Philos Trans R Soc Lond Ser A Math Phys Eng Sci 357(1751):335–353. https://doi.org/10.1098/rsta.1999.0330
161. Dolores R, Raquel S, Adianez G-L (2015) Sonochemical synthesis of iron oxide nanoparticles loaded with folate and cisplatin: effect of ultrasonic frequency. Ultrason Sonochem 23:391–398. https://doi.org/10.1016/j.ultsonch.2014.08.005
162. Shafi KVPM, Ulman A, Yan X, Yang N-L, Estournès C, White H, Rafailovich M (2001) Sonochemical synthesis of functionalized amorphous iron oxide nanoparticles. Langmuir 17(16):5093–5097. https://doi.org/10.1021/la010421+
163. Vijayakumar R, Koltypin Y, Felner I, Gedanken A (2000) Sonochemical synthesis and characterization of pure nanometer-sized Fe_3O_4 particles. Mater Sci Eng A 286(1):101–105. https://doi.org/10.1016/S0921-5093(00)00647-X
164. Abu Mukh-Qasem R, Gedanken A (2005) Sonochemical synthesis of stable hydrosol of Fe_3O_4 nanoparticles. J Colloid Interface Sci 284(2):489–494. https://doi.org/10.1016/j.jcis.2004.10.073
165. Rahmawati R, Kaneti YV, Taufiq A, Sunaryono YB, Suyatman N, Kurniadi D, Hossain MSA, Yamauchi Y (2018) Green synthesis of magnetite nanostructures from naturally available iron sands via sonochemical method. Bull Chem Soc Jpn 91(2):311–317. https://doi.org/10.1246/bcsj.20170317
166. Hee Kim E, Sook Lee H, Kook Kwak B, Kim B-K (2005) Synthesis of ferrofluid with magnetic nanoparticles by sonochemical method for MRI contrast agent. J Magn Magn Mater 289:328–330. https://doi.org/10.1016/j.jmmm.2004.11.093
167. Abbas M, Torati SR, Kim C (2015) A novel approach for the synthesis of ultrathin silica-coated iron oxide nanocubes decorated with silver nanodots ($Fe_3O_4/SiO_2/Ag$) and their superior catalytic reduction of 4-nitroaniline. Nanoscale 7(28):12192–12204. https://doi.org/10.1039/C5NR02680F
168. Shafi KVPM, Koltypin Y, Gedanken A, Prozorov R, Balogh J, Lendvai J, Felner I (1997) Sonochemical preparation of nanosized amorphous $NiFe_2O_4$ particles. J Phys Chem B 101(33):6409–6414. https://doi.org/10.1021/jp970893q
169. Shafi KVPM, Gedanken A, Prozorov R, Balogh J (1998) Sonochemical preparation and size-dependent properties of nanostructured $CoFe_2O_4$ particles. Chem Mater 10(11):3445–3450. https://doi.org/10.1021/cm980182k
170. Sodipo BK, Aziz AA (2018) One minute synthesis of amino-silane functionalized superparamagnetic iron oxide nanoparticles by sonochemical method. Ultrason Sonochem 40:837–840. https://doi.org/10.1016/j.ultsonch.2017.08.040
171. Sathya A, Kalyani S, Ranoo S, Philip J (2017) One-step microwave-assisted synthesis of water-dispersible Fe_3O_4 magnetic nanoclusters for hyperthermia applications. J Magn Magn Mater 439:107–113. https://doi.org/10.1016/j.jmmm.2017.05.018
172. Palchik O, Felner I, Kataby G, Gedanken A (2011) Amorphous iron oxide prepared by microwave heating. J Mater Res 15(10):2176–2181. https://doi.org/10.1557/JMR.2000.0313
173. Liu Z, Miao F, Hua W, Zhao F (2012) Fe_3O_4 nanoparticles: microwave-assisted synthesis and mechanism. Mater Lett 67(1):358–361. https://doi.org/10.1016/j.matlet.2011.09.095
174. Kostyukhin EM, Kustov LM (2018) Microwave-assisted synthesis of magnetite nanoparticles possessing superior magnetic properties. Mendeleev Commun 28(5):559–561. https://doi.org/10.1016/j.mencom.2018.09.038
175. Bonfim L, de Queiroz Souza PP, de Oliveira Gonçalves K, Courrol LC, de Oliveira Silva FR, Vieira DP (2019) Microwave-mediated synthesis of iron-oxide nanoparticles for use in magnetic levitation cell cultures. Appl Nanosci 9(8):1707–1717. https://doi.org/10.1007/s13204-019-00962-1
176. Aivazoglou E, Metaxa E, Hristoforou E (2017) Microwave-assisted synthesis of iron oxide nanoparticles in biocompatible organic environment. AIP Adv 8(4):048201. https://doi.org/10.1063/1.4994057
177. Lastovina TA, Budnyk AP, Soldatov MA, Rusalev YV, Guda AA, Bogdan AS, Soldatov AV (2017) Microwave-assisted synthesis of magnetic iron oxide nanoparticles in oleylamine–oleic acid solutions. Mendeleev Commun 27(5):487–489. https://doi.org/10.1016/j.mencom.2017.09.019

178. Cao S-W, Zhu Y-J (2009) Iron oxide hollow spheres: microwave–hydrothermal ionic liquid preparation, formation mechanism, crystal phase and morphology control and properties. Acta Mater 57(7):2154–2165. https://doi.org/10.1016/j.actamat.2009.01.009
179. Blanco-Andujar C, Ortega D, Southern P, Pankhurst QA, Thanh NTK (2015) High performance multi-core iron oxide nanoparticles for magnetic hyperthermia: microwave synthesis, and the role of core-to-core interactions. Nanoscale 7(5):1768–1775. https://doi.org/10.1039/C4NR06239F
180. Jiang FY, Wang CM, Fu Y, Liu RC (2010) Synthesis of iron oxide nanocubes via microwave-assisted solvolthermal method. J Alloy Compd 503(2):L31–L33. https://doi.org/10.1016/j.jallcom.2010.05.020
181. Hu L, Percheron A, Chaumont D, Brachais C-H (2011) Microwave-assisted one-step hydrothermal synthesis of pure iron oxide nanoparticles: magnetite, maghemite and hematite. J Sol-Gel Sci Technol 60(2):198. https://doi.org/10.1007/s10971-011-2579-4
182. Wu L, Yao H, Hu B, Yu S-H (2011) Unique lamellar sodium/potassium iron oxide nanosheets: facile microwave-assisted synthesis and magnetic and electrochemical properties. Chem Mater 23(17):3946–3952. https://doi.org/10.1021/cm2013736
183. Katsuki H, Choi E-K, Lee W-J, Hwang K-T, Cho W-S, Huang W, Komarneni S (2018) Ultrafast microwave-hydrothermal synthesis of hexagonal plates of hematite. Mater Chem Phys 205:210–216. https://doi.org/10.1016/j.matchemphys.2017.10.078
184. Fernández-Barahona I, Gutiérrez L, Veintemillas-Verdaguer S, Pellico J, Morales MdP, Catala M, del Pozo MA, Ruiz-Cabello J, Herranz F (2019) Cu-doped extremely small iron oxide nanoparticles with large longitudinal relaxivity: one-pot synthesis and in vivo targeted molecular imaging. ACS Omega 4(2):2719–2727. https://doi.org/10.1021/acsomega.8b03004
185. Hong RY, Pan TT, Li HZ (2006) Microwave synthesis of magnetic Fe_3O_4 nanoparticles used as a precursor of nanocomposites and ferrofluids. J Magn Magn Mater 303(1):60–68. https://doi.org/10.1016/j.jmmm.2005.10.230
186. Katsuki H, Komarneni S (2001) Microwave-hydrothermal synthesis of monodispersed nanophase α-Fe_2O_3. J Am Ceram Soc 84(10):2313–2317. https://doi.org/10.1111/j.1151-2916.2001.tb01007.x
187. Pascu O, Carenza E, Gich M, Estradé S, Peiró F, Herranz G, Roig A (2012) Surface reactivity of iron oxide nanoparticles by microwave-assisted synthesis; comparison with the thermal decomposition route. J Phys Chem C 116(28):15108–15116. https://doi.org/10.1021/jp303204d
188. Xiao W, Gu H, Li D, Chen D, Deng X, Jiao Z, Lin J (2012) Microwave-assisted synthesis of magnetite nanoparticles for MR blood pool contrast agents. J Magn Magn Mater 324(4):488–494. https://doi.org/10.1016/j.jmmm.2011.08.029
189. Carenza E, Barceló V, Morancho A, Montaner J, Rosell A, Roig A (2014) Rapid synthesis of water-dispersible superparamagnetic iron oxide nanoparticles by a microwave-assisted route for safe labeling of endothelial progenitor cells. Acta Biomater 10(8):3775–3785. https://doi.org/10.1016/j.actbio.2014.04.010
190. Narayanan KB, Sakthivel N (2010) Biological synthesis of metal nanoparticles by microbes. Adv Coll Interface Sci 156(1):1–13. https://doi.org/10.1016/j.cis.2010.02.001
191. Shah M, Fawcett D, Sharma S, Tripathy KS, Poinern EG (2015) Green synthesis of metallic nanoparticles via biological entities. Materials 8:11. https://doi.org/10.3390/ma8115377
192. Lovley DR, Stolz JF, Nord GL, Phillips EJP (1987) Anaerobic production of magnetite by a dissimilatory iron-reducing microorganism. Nature 330(6145):252–254. https://doi.org/10.1038/330252a0
193. Zhang C, Vali H, Romanek CS, Phelps TJ, Liu SV (1998) Formation of single-domain magnetite by a thermophilic bacterium. Am Mineral 83(11–12_Part_2):1409–1418. https://doi.org/10.2138/am-1998-11-1230
194. Philipse AP, Maas D (2002) Magnetic colloids from magnetotactic bacteria: chain formation and colloidal stability. Langmuir 18(25):9977–9984. https://doi.org/10.1021/la0205811
195. Lee H, Purdon AM, Chu V, Westervelt RM (2004) Controlled assembly of magnetic nanoparticles from magnetotactic bacteria using microelectromagnets arrays. Nano Lett 4(5):995–998. https://doi.org/10.1021/nl049562x
196. Lang C, Schüler D (2006) Biogenic nanoparticles: production, characterization, and application of bacterial magnetosomes. J Phys Condens Matter 18(38):S2815–S2828. https://doi.org/10.1088/0953-8984/18/38/s19
197. Lisy MR, Hartung A, Lang C, Schuler D, Richter W, Reichenbach JR, Kaiser WA, Hilger I (2007) Fluorescent bacterial magnetic nanoparticles as bimodal contrast agents. Invest Radiol 42(4):235–241. https://doi.org/10.1097/01.rli.0000255832.44443.e7

198. Bharde A, Wani A, Shouche Y, Joy PA, Prasad BLV, Sastry M (2005) Bacterial aerobic synthesis of nanocrystalline magnetite. J Am Chem Soc 127(26):9326–9327. https://doi.org/10.1021/ja058469
199. Bharde AA, Parikh RY, Baidakova M, Jouen S, Hannoyer B, Enoki T, Prasad BLV, Shouche YS, Ogale S, Sastry M (2008) Bacteria-mediated precursor-dependent biosynthesis of superparamagnetic iron oxide and iron sulfide nanoparticles. Langmuir 24(11):5787–5794. https://doi.org/10.1021/la704019p
200. Bharde A, Rautaray D, Bansal V, Ahmad A, Sarkar I, Yusuf SM, Sanyal M, Sastry M (2006) Extracellular biosynthesis of magnetite using fungi. Small 2(1):135–141. https://doi.org/10.1002/smll.200500180
201. Shenton W, Douglas T, Young M, Stubbs G, Mann S (1999) Inorganic–organic nanotube composites from template mineralization of tobacco mosaic virus. Adv Mater 11(3):253–256. https://doi.org/10.1002/(SICI)1521-4095(199903)11:3%3c253:AID-ADMA253%3e3.0.CO;2-7
202. Aeppli M, Kaegi R, Kretzschmar R, Voegelin A, Hofstetter TB, Sander M (2019) Electrochemical analysis of changes in iron oxide reducibility during abiotic ferrihydrite transformation into goethite and magnetite. Environ Sci Technol 53(7):3568–3578. https://doi.org/10.1021/acs.est.8b07190
203. Moon J-W, Rawn CJ, Rondinone AJ, Love LJ, Roh Y, Everett SM, Lauf RJ, Phelps TJ (2010) Large-scale production of magnetic nanoparticles using bacterial fermentation. J Ind Microbiol Biotechnol 37(10):1023–1031. https://doi.org/10.1007/s10295-010-0749-y
204. Iravani S (2011) Green synthesis of metal nanoparticles using plants. Green Chem 13(10):2638–2650. https://doi.org/10.1039/C1GC15386B
205. Aksu Demirezen D, Yıldız YŞ, Yılmaz Ş, Demirezen Yılmaz D (2019) Green synthesis and characterization of iron oxide nanoparticles using *Ficus carica* (common fig) dried fruit extract. J Biosci Bioeng 127(2):241–245. https://doi.org/10.1016/j.jbiosc.2018.07.024
206. Lohrasbi S, Kouhbanani MAJ, Beheshtkhoo N, Ghasemi Y, Amani AM, Taghizadeh S (2019) Green synthesis of iron nanoparticles using plantago major leaf extract and their application as a catalyst for the decolorization of azo dye. BioNanoScience 9(2):317–322. https://doi.org/10.1007/s12668-019-0596-x
207. Salazar-Alvarez G, Muhammed M, Zagorodni AA (2006) Novel flow injection synthesis of iron oxide nanoparticles with narrow size distribution. Chem Eng Sci 61(14):4625–4633. https://doi.org/10.1016/j.ces.2006.02.032
208. Dierstein A, Natter H, Meyer F, Stephan HO, Kropf C, Hempelmann R (2001) Electrochemical deposition under oxidizing conditions (EDOC): a new synthesis for nanocrystalline metal oxides. Scripta Mater 44(8):2209–2212. https://doi.org/10.1016/S1359-6462(01)00906-X
209. Pascal C, Pascal JL, Favier F, Elidrissi Moubtassim ML, Payen C (1999) Electrochemical synthesis for the control of γ-Fe2O3 nanoparticle size. Morphology, microstructure, and magnetic behavior. Chem Mater 11(1):141–147. https://doi.org/10.1021/cm980742f
210. Ramimoghadam D, Bagheri S, Hamid SBA (2014) Progress in electrochemical synthesis of magnetic iron oxide nanoparticles. J Magn Magn Mater 368:207–229. https://doi.org/10.1016/j.jmmm.2014.05.015
211. Carraro G, Barreca D, Maccato C, Bontempi E, Depero LE, de Julián FC, Caneschi A (2013) Supported ε and β iron oxide nanomaterials by chemical vapor deposition: structure, morphology and magnetic properties. CrystEngComm 15(6):1039–1042. https://doi.org/10.1039/C2CE26821C
212. Alijani H, Beyki MH, Shariatinia Z, Bayat M, Shemirani F (2014) A new approach for one step synthesis of magnetic carbon nanotubes/diatomite earth composite by chemical vapor deposition method: application for removal of lead ions. Chem Eng J 253:456–463. https://doi.org/10.1016/j.cej.2014.05.021
213. Morjan I, Alexandrescu R, Dumitrache F, Birjega R, Fleaca C, Soare I, Luculescu CR, Filoti G, Kuncer V, Vekas L, Popa NC, Prodan G, Ciupina V (2010) Iron oxide-based nanoparticles with different mean sizes obtained by the laser pyrolysis: structural and magnetic properties. J Nanosci Nanotechnol 10(2):1223–1234. https://doi.org/10.1166/jnn.2010.1863
214. Dinesha ML, Jayanna HS, Mohanty S, Ravi S (2010) Structural, electrical and magnetic properties of Co and Fe co-doped ZnO nanoparticles prepared by solution combustion method. J Alloy Compd 490(1):618–623. https://doi.org/10.1016/j.jallcom.2009.10.120
215. Ma J, Lee SM-Y, Yi C, Li C-W (2017) Controllable synthesis of functional nanoparticles by microfluidic platforms for biomedical applications—a review. Lab Chip 17(2):209–226. https://doi.org/10.1039/C6LC01049K

216. Hwang DK, Dendukuri D, Doyle PS (2008) Microfluidic-based synthesis of non-spherical magnetic hydrogel microparticles. Lab Chip 8(10):1640–1647. https://doi.org/10.1039/B805176C
217. Wei J, Shuai X, Wang R, He X, Li Y, Ding M, Li J, Tan H, Fu Q (2017) Clickable and imageable multiblock polymer micelles with magnetically guided and PEG-switched targeting and release property for precise tumor theranosis. Biomaterials 145:138–153. https://doi.org/10.1016/j.biomaterials.2017.08.005
218. Li H, Yan K, Shang Y, Shrestha L, Liao R, Liu F, Li P, Xu H, Xu Z, Chu PK (2015) Folate-bovine serum albumin functionalized polymeric micelles loaded with superparamagnetic iron oxide nanoparticles for tumor targeting and magnetic resonance imaging. Acta Biomater 15:117–126. https://doi.org/10.1016/j.actbio.2015.01.006
219. Starmans LWE, Moonen RPM, Aussems-Custers E, Daemen MJAP, Strijkers GJ, Nicolay K, Grüll H (2015) Evaluation of iron oxide nanoparticle micelles for magnetic particle imaging (MPI) of thrombosis. PLoS ONE 10:3. https://doi.org/10.1371/journal.pone.0119257
220. Xiao S, Castro R, Rodrigues J, Shi X, Tomá H (2014) PAMAM dendrimer/pDNA functionalized-magnetic iron oxide nanoparticles for gene delivery. J Biomed Nanotechnol 11(8):1418–1430. https://doi.org/10.1166/jbn.2015.2101
221. Upponi JR, Jerajani K, Nagesha DK, Kulkarni P, Sridhar S, Ferris C, Torchilin VP (2018) Polymeric micelles: theranostic co-delivery system for poorly water-soluble drugs and contrast agents. Biomaterials 170:26–36. https://doi.org/10.1016/j.biomaterials.2018.03.054
222. Tsai CH, Tang YH, Chen HT, Yao YW, Chien TC, Kao CL (2018) A selective glucose sensor: the cooperative effect of monoboronic acid-modified poly(amidoamine) dendrimers. Chem Commun 54(36):4577–4580. https://doi.org/10.1039/c8cc00914g
223. Babamiri B, Hallaj R, Salimi A (2018) Ultrasensitive electrochemiluminescence immunoassay for simultaneous determination of CA125 and CA15-3 tumor markers based on PAMAM-sulfanilic acid-Ru(bpy)32+ and PAMAM-CdTe@CdS nanocomposite. Biosens Bioelectron 99:353–360. https://doi.org/10.1016/j.bios.2017.07.062
224. Wang G, Fu L, Walker A, Chen X, Lovejoy DB, Hao M, Lee A, Chung R, Rizos H, Irvine M, Zheng M, Liu X, Lu Y, Shi B (2019) Label-free fluorescent poly(amidoamine) dendrimer for traceable and controlled drug delivery. Biomacromol 20(5):2148–2158. https://doi.org/10.1021/acs.biomac.9b00494
225. Najafi F, Salami-Kalajahi M, Roghani-Mamaqani H, Kahaie-Khosrowshahi A (2019) Effect of grafting ratio of poly(propylene imine) dendrimer onto gold nanoparticles on the properties of colloidal hybrids, their DOX loading and release behavior and cytotoxicity. Colloids Surf B 178:500–507. https://doi.org/10.1016/j.colsurfb.2019.03.050
226. Wang B, Sun Y, Davis TP, Ke PC, Wu Y, Ding F (2018) Understanding effects of PAMAM dendrimer size and surface chemistry on serum protein binding with discrete molecular dynamics simulations. ACS Sustain Chem Eng 6(9):11704–11715. https://doi.org/10.1021/acssuschemeng.8b01959
227. Tian F, Lin X, Valle RP, Zuo YY, Gu N (2019) Poly(amidoamine) dendrimer as a respiratory nanocarrier: insights from experiments and molecular dynamics simulations. Langmuir 35(15):5364–5371. https://doi.org/10.1021/acs.langmuir.9b00434
228. Jędrzak A, Grześkowiak BF, Coy E, Wojnarowicz J, Szutkowski K, Jurga S, Jesionowski T, Mrówczyński R (2019) Dendrimer based theranostic nanostructures for combined chemo- and photothermal therapy of liver cancer cells in vitro. Colloids Surf B 173:698–708. https://doi.org/10.1016/j.colsurfb.2018.10.045
229. Luong D, Sau S, Kesharwani P, Iyer AK (2017) Polyvalent Folate–Dendrimer-coated iron oxide theranostic nanoparticles for simultaneous magnetic resonance imaging and precise cancer cell targeting. Biomacromol 18(4):1197–1209. https://doi.org/10.1021/acs.biomac.6b01885
230. Shirmardi Shaghasemi B, Virk MM, Reimhult E (2017) Optimization of magneto-thermally controlled release kinetics by tuning of magnetoliposome composition and structure. Sci Rep 7:1. https://doi.org/10.1038/s41598-017-06980-9
231. German SV, Navolokin NA, Kuznetsova NR, Zuev VV, Inozemtseva OA, Anis'kov AA, Volkova EK, Bucharskaya AB, Maslyakova GN, Fakhrullin RF, Terentyuk GS, Vodovozova EL, Gorin DA (2015) Liposomes loaded with hydrophilic magnetite nanoparticles: preparation and application as contrast agents for magnetic resonance imaging. Colloids SurfB 135:109–115. https://doi.org/10.1016/j.colsurfb.2015.07.042

232. Cuomo F, Cofelice M, Venditti F, Ceglie A, Miguel M, Lindman B, Lopez F (2018) In-vitro digestion of curcumin loaded chitosan-coated liposomes. Colloids Surf B 168:29–34. https://doi.org/10.1016/j.colsurfb.2017.11.047
233. Di Corato R, Béalle G, Kolosnjaj-Tabi J, Espinosa A, Clément O, Silva AKA, Ménager C, Wilhelm C (2015) Combining magnetic hyperthermia and photodynamic therapy for tumor ablation with photoresponsive magnetic liposomes. ACS Nano 9(3):2904–2916. https://doi.org/10.1021/nn506949t
234. Zheng XC, Ren W, Zhang S, Zhong T, Duan XC, Yin YF, Xu MQ, Hao YL, Li ZT, Li H, Liu M, Li ZY, Zhang X (2018) The theranostic efficiency of tumor-specific, pH-responsive, peptide-modified, liposome-containing paclitaxel and superparamagnetic iron oxide nanoparticles. Int J Nanomed 13:1495–1504. https://doi.org/10.2147/IJN.S157082
235. Caro C, García-Martín ML, Pernia Leal M (2017) Manganese-based nanogels as pH switches for magnetic resonance imaging. Biomacromol 18(5):1617–1623. https://doi.org/10.1021/acs.biomac.7b00224
236. Riedinger A, Pernia Leal M, Deka SR, George C, Franchini IR, Falqui A, Cingolani R, Pellegrino T (2011) "nanohybrids" based on pH-responsive hydrogels and inorganic nanoparticles for drug delivery and sensor applications. Nano Lett 11(8):3136–3141
237. Jalili NA, Jaiswal MK, Peak CW, Cross LM, Gaharwar AK (2017) Injectable nanoengineered stimuli-responsive hydrogels for on-demand and localized therapeutic delivery. Nanoscale 9(40):15379–15389. https://doi.org/10.1039/c7nr02327h
238. Peng N, Ding X, Wang Z, Cheng Y, Gong Z, Xu X, Gao X, Cai Q, Huang S, Liu Y (2019) Novel dual responsive alginate-based magnetic nanogels for onco-theranostics. Carbohyd Polym 204:32–41. https://doi.org/10.1016/j.carbpol.2018.09.084
239. Li W, Xue B, Shi K, Qu Y, Chu B, Qian Z (2019) Magnetic iron oxide nanoparticles/10-hydroxy camptothecin co-loaded nanogel for enhanced photothermal-chemo therapy. Appl Mater Today 14:84–95. https://doi.org/10.1016/j.apmt.2018.11.008
240. Sun W, Yang J, Zhu J, Zhou Y, Li J, Zhu X, Shen M, Zhang G, Shi X (2016) Immobilization of iron oxide nanoparticles within alginate nanogels for enhanced MR imaging applications. Biomater Sci 4(10):1422–1430. https://doi.org/10.1039/c6bm00370b
241. Hao X, Xu B, Chen H, Wang X, Zhang J, Guo R, Shi X, Cao X (2019) Stem cell-mediated delivery of nanogels loaded with ultrasmall iron oxide nanoparticles for enhanced tumor MR imaging. Nanoscale 11(11):4904–4910. https://doi.org/10.1039/c8nr10490e
242. Hwang J, Lee E, Kim J, Seo Y, Lee KH, Hong JW, Gilad AA, Park H, Choi J (2016) Effective delivery of immunosuppressive drug molecules by silica coated iron oxide nanoparticles. Colloids Surf B 142:290–296. https://doi.org/10.1016/j.colsurfb.2016.01.040
243. Monaco I, Arena F, Biffi S, Locatelli E, Bortot B, La Cava F, Marini GM, Severini GM, Terreno E, Comes Franchini M (2017) Synthesis of lipophilic core-shell Fe_3O_4@SiO_2@Au nanoparticles and polymeric entrapment into nanomicelles: a novel nanosystem for in vivo active targeting and magnetic resonance-photoacoustic dual imaging. Bioconjug Chem 28(5):1382–1390. https://doi.org/10.1021/acs.bioconjchem.7b00076
244. Guisasola E, Asín L, Beola L, de la Fuente JM, Baeza A, Vallet-Regí M (2018) Beyond traditional hyperthermia: in vivo cancer treatment with magnetic-responsive mesoporous silica nanocarriers. ACS Appl Mater Interfaces 10(15):12518–12525. https://doi.org/10.1021/acsami.8b02398
245. Hurley KR, Ring HL, Etheridge M, Zhang J, Gao Z, Shao Q, Klein ND, Szlag VM, Chung C, Reineke TM, Garwood M, Bischof JC, Haynes CL (2016) Predictable heating and positive MRI contrast from a mesoporous silica-coated iron oxide nanoparticle. Mol Pharm 13(7):2172–2183. https://doi.org/10.1021/acs.molpharmaceut.5b00866
246. Park W, Yang HN, Ling D, Yim H, Kim KS, Hyeon T, Na K, Park KH (2014) Multi-modal transfection agent based on monodisperse magnetic nanoparticles for stem cell gene delivery and tracking. Biomaterials 35(25):7239–7247. https://doi.org/10.1016/j.biomaterials.2014.05.010
247. Lassenberger A, Bixner O, Gruenewald T, Lichtenegger H, Zirbs R, Reimhult E (2016) Evaluation of high-yield purification methods on monodisperse PEG-grafted iron oxide nanoparticles. Langmuir 32(17):4259–4269. https://doi.org/10.1021/acs.langmuir.6b00919
248. Pernia Leal M, Rivera-Fernández S, Franco JM, Pozo D, de la Fuente JM, García-Martín ML (2015) Long-circulating PEGylated manganese ferrite nanoparticles for MRI-based molecular imaging. Nanoscale 7(5):2050–2059. https://doi.org/10.1039/C4NR05781C

249. Pernia Leal M, Caro C, García-Martín ML (2017) Shedding light on zwitterionic magnetic nanoparticles: limitations for in vivo applications. Nanoscale 9(24):8176–8184. https://doi.org/10.1039/C7NR01607G
250. Leal MP, Muñoz-Hernández C, Berry CC, García-Martín ML (2015) In vivo pharmacokinetics of T2 contrast agents based on iron oxide nanoparticles: optimization of blood circulation times. RSC Adv 5(94):76883–76891. https://doi.org/10.1039/C5RA15680G
251. Weissleder R, Mahmood U (2001) Molecular imaging. Radiology 219(2):316–333. https://doi.org/10.1148/radiology.219.2.r01ma19316
252. Torrey HC (1956) Bloch equations with diffusion terms. Phys Rev 104(3):563–565. https://doi.org/10.1103/PhysRev.104.563
253. Enriquez-Navas PM, Garcia-Martin ML (2012) Chapter 9—application of inorganic nanoparticles for diagnosis based on MRI. In: de la Fuente JM, Grazu V (eds) Frontiers of nanoscience, vol 4. Elsevier, Oxford, pp 233–245. https://doi.org/10.1016/B978-0-12-415769-9.00009-1
254. Geraldes CF, Laurent S (2009) Classification and basic properties of contrast agents for magnetic resonance imaging. Contrast Media Mol Imaging 4(1):1–23. https://doi.org/10.1002/cmmi.265
255. Yan G-P, Robinson L, Hogg P (2007) Magnetic resonance imaging contrast agents: overview and perspectives. Radiography 13:e5–e19. https://doi.org/10.1016/j.radi.2006.07.005
256. Bridot J-L, Faure A-C, Laurent S, Rivière C, Billotey C, Hiba B, Janier M, Josserand V, Coll J-L, Vander Elst L, Muller R, Roux S, Perriat P, Tillement O (2007) Hybrid gadolinium oxide nanoparticles: multimodal contrast agents for in vivo imaging. J Am Chem Soc 129(16):5076–5084. https://doi.org/10.1021/ja068356j
257. Ersoy H, Rybicki FJ (2007) Biochemical safety profiles of gadolinium-based extracellular contrast agents and nephrogenic systemic fibrosis. J Magn Reson Imaging 26(5):1190–1197. https://doi.org/10.1002/jmri.21135
258. Dias MHM, Lauterbur PC (1986) Ferromagnetic particles as contrast agents for magnetic resonance imaging of liver and spleen. Magn Reson Med 3(2):328–330. https://doi.org/10.1002/mrm.1910030218
259. Kim MP, Evans DB, Wang H, Abbruzzese JL, Fleming JB, Gallick GE (2009) Generation of orthotopic and heterotopic human pancreatic cancer xenografts in immunodeficient mice. Nat Protoc 4(11):1670–1680. https://doi.org/10.1038/nprot.2009.171
260. Jin K, Teng L, Shen Y, He K, Xu Z, Li G (2010) Patient-derived human tumour tissue xenografts in immunodeficient mice: a systematic review. Clin Transl Oncol 12(7):473–480. https://doi.org/10.1007/s12094-010-0540-6
261. Carlos C, David P (2015) Polysaccharide colloids as smart vehicles in cancer therapy. Curr Pharm Des 21(33):4822–4836. https://doi.org/10.2174/1381612821666150820100812
262. Efremova MV, Naumenko VA, Spasova M, Garanina AS, Abakumov MA, Blokhina AD, Melnikov PA, Prelovskaya AO, Heidelmann M, Li Z-A, Ma Z, Shchetinin IV, Golovin YI, Kireev II, Savchenko AG, Chekhonin VP, Klyachko NL, Farle M, Majouga AG, Wiedwald U (2018) Magnetite–gold nanohybrids as ideal all-in-one platforms for theranostics. Sci Rep 8(1):11295. https://doi.org/10.1038/s41598-018-29618-w
263. Li Y, Song K, Cao Y, Peng C, Yang G (2018) Keratin-templated synthesis of metallic oxide nanoparticles as MRI contrast agents and drug carriers. ACS Appl Mater Interfaces 10(31):26039–26045. https://doi.org/10.1021/acsami.8b08555
264. Hsu JC, Naha PC, Lau KC, Chhour P, Hastings R, Moon BF, Stein JM, Witschey WRT, McDonald ES, Maidment ADA, Cormode DP (2018) An all-in-one nanoparticle (AION) contrast agent for breast cancer screening with DEM-CT-MRI-NIRF imaging. Nanoscale 10(36):17236–17248. https://doi.org/10.1039/C8NR03741H
265. Ren S, Yang J, Ma L, Li X, Wu W, Liu C, He J, Miao L (2018) Ternary-responsive drug delivery with activatable dual mode contrast-enhanced in vivo imaging. ACS Appl Mater Interfaces 10(38):31947–31958. https://doi.org/10.1021/acsami.8b10564
266. Shirvalilou S, Khoei S, Khoee S, Raoufi NJ, Karimi MR, Shakeri-Zadeh A (2018) Development of a magnetic nano-graphene oxide carrier for improved glioma-targeted drug delivery and imaging: In vitro and in vivo evaluations. Chem Biol Interact 295:97–108. https://doi.org/10.1016/j.cbi.2018.08.027
267. Sun J, Xu W, Li L, Fan B, Peng X, Qu B, Wang L, Li T, Li S, Zhang R (2018) Ultrasmall endogenous biopolymer nanoparticles for magnetic resonance/photoacoustic dual-modal imaging-guided photothermal therapy. Nanoscale 10(22):10584–10595. https://doi.org/10.1039/C8NR01215F

268. Thirunavukkarasu GK, Cherukula K, Lee H, Jeong YY, Park I-K, Lee JY (2018) Magnetic field-inducible drug-eluting nanoparticles for image-guided thermo-chemotherapy. Biomaterials 180:240–252. https://doi.org/10.1016/j.biomaterials.2018.07.028
269. Zhang J, Mu Y-L, Ma Z-Y, Han K, Han H-Y (2018) Tumor-triggered transformation of chimeric peptide for dual-stage-amplified magnetic resonance imaging and precise photodynamic therapy. Biomaterials 182:269–278. https://doi.org/10.1016/j.biomaterials.2018.08.026
270. Sosnovik DE, Weissleder R (2007) Emerging concepts in molecular MRI. Curr Opin Biotechnol 18(1):4–10. https://doi.org/10.1016/j.copbio.2006.11.001
271. Klausner RD (1996) The future of cancer research and the role of the National Cancer Institute. J Clin Oncol 14(10):2878–2883. https://doi.org/10.1200/JCO.1996.14.10.2878
272. Gillies RJ (2002) In vivo molecular imaging. J Cell Biochem 87(S39):231–238. https://doi.org/10.1002/jcb.10450
273. Reimer P, Weissleder R, Lee AS, Wittenberg J, Brady TJ (1990) Receptor imaging: application to MR imaging of liver cancer. Radiology 177(3):729–734. https://doi.org/10.1148/radiology.177.3.2243978
274. Tsoukalas C, Psimadas D, Kastis GA, Koutoulidis V, Harris AL, Paravatou-Petsotas M, Karageorgou M, Furenlid LR, Moulopoulos LA, Stamopoulos D, Bouziotis P (2018) A novel metal-based imaging probe for targeted dual-modality SPECT/MR imaging of angiogenesis. Front Chem 6:224–224. https://doi.org/10.3389/fchem.2018.00224
275. Ding N, Sano K, Kanazaki K, Ohashi M, Deguchi J, Kanada Y, Ono M, Saji H (2016) In vivo HER2-targeted magnetic resonance tumor imaging using iron oxide nanoparticles conjugated with anti-HER2 fragment antibody. Mol Imag Biol 18(6):870–876. https://doi.org/10.1007/s11307-016-0977-2
276. Ge Y, Zhong Y, Ji G, Lu Q, Dai X, Guo Z, Zhang P, Peng G, Zhang K, Li Y (2018) Preparation and characterization of Fe_3O_4@Au-C225 composite targeted nanoparticles for MRI of human glioma. PLoS ONE 13(4):e0195703–e0195703. https://doi.org/10.1371/journal.pone.0195703
277. Conde J, Bao C, Cui D, Baptista PV, Tian F (2014) Antibody–drug gold nanoantennas with Raman spectroscopic fingerprints for in vivo tumour theranostics. J Control Release 183:87–93. https://doi.org/10.1016/j.jconrel.2014.03.045
278. Zarschler K, Prapainop K, Mahon E, Rocks L, Bramini M, Kelly PM, Stephan H, Dawson KA (2014) Diagnostic nanoparticle targeting of the EGF-receptor in complex biological conditions using single-domain antibodies. Nanoscale 6(11):6046–6056. https://doi.org/10.1039/C4NR00595C
279. Shevtsov MA, Nikolaev BP, Yakovleva LY, Marchenko YY, Dobrodumov AV, Mikhrina AL, Martynova MG, Bystrova OA, Yakovenko IV, Ischenko AM (2014) Superparamagnetic iron oxide nanoparticles conjugated with epidermal growth factor (SPION-EGF) for targeting brain tumors. Int J Nanomed 9:273–287. https://doi.org/10.2147/IJN.S55118
280. Ren J, Zhang Z, Wang F, Yang Y, Liu Y, Wei G, Yang A, Zhang R, Huan Y, Cui Y, Larson AC (2012) MRI of prostate stem cell antigen expression in prostate tumors. Nanomedicine 7(5):691–703. https://doi.org/10.2217/nnm.11.147
281. Gottschalk K-E, Kessler H (2002) The structures of integrins and integrin–ligand complexes: implications for drug design and signal transduction. Angew Chem Int Ed 41(20):3767–3774. https://doi.org/10.1002/1521-3773(20021018)41:20%3c3767:AID-ANIE3767%3e3.0.CO;2-T
282. Akhtar MJ, Ahamed M, Alhadlaq HA, Alrokayan SA, Kumar S (2014) Targeted anticancer therapy: overexpressed receptors and nanotechnology. Clin Chim Acta 436:78–92. https://doi.org/10.1016/j.cca.2014.05.004
283. Yameen B, Choi WI, Vilos C, Swami A, Shi J, Farokhzad OC (2014) Insight into nanoparticle cellular uptake and intracellular targeting. J Control Release 190:485–499. https://doi.org/10.1016/j.jconrel.2014.06.038
284. Chen K, Xie J, Xu H, Behera D, Michalski MH, Biswal S, Wang A, Chen X (2009) Triblock copolymer coated iron oxide nanoparticle conjugate for tumor integrin targeting. Biomaterials 30(36):6912–6919. https://doi.org/10.1016/j.biomaterials.2009.08.045
285. Chen L, Xie J, Wu H, Zang F, Ma M, Hua Z, Gu N, Zhang Y (2018) Improving sensitivity of magnetic resonance imaging by using a dual-targeted magnetic iron oxide nanoprobe. Colloids Surf B Biointerfaces 161:339–346. https://doi.org/10.1016/j.colsurfb.2017.10.059
286. Sánchez A, Ovejero Paredes K, Ruiz-Cabello J, Martínez-Ruíz P, Pingarrón JM, Villalonga R, Filice M (2018) Hybrid decorated core@shell janus nanoparticles as a flexible

platform for targeted multimodal molecular bioimaging of cancer. ACS Appl Mater Interfaces 10(37):31032–31043. https://doi.org/10.1021/acsami.8b10452
287. Li J, Wu C, Hou P, Zhang M, Xu K (2018) One-pot preparation of hydrophilic manganese oxide nanoparticles as T1 nano-contrast agent for molecular magnetic resonance imaging of renal carcinoma in vitro and in vivo. Biosens Bioelectron 102:1–8. https://doi.org/10.1016/j.bios.2017.10.047
288. Zhao M, Liu Z, Dong L, Zhou H, Yang S, Wu W, Lin J (2018) A GPC3-specific aptamer-mediated magnetic resonance probe for hepatocellular carcinoma. Int J Nanomed 13:4433–4443. https://doi.org/10.2147/IJN.S168268
289. Zhu Y, Sun Y, Chen Y, Liu W, Jiang J, Guan W, Zhang Z, Duan Y (2015) In vivo molecular MRI imaging of prostate cancer by targeting PSMA with polypeptide-labeled superparamagnetic iron oxide nanoparticles. Int J Mol Sci 16(5):9573–9587. https://doi.org/10.3390/ijms16059573
290. Wang G, Qian K, Mei X (2018) A theranostic nanoplatform: magneto-gold@fluorescence polymer nanoparticles for tumor targeting T1&T2-MRI/CT/NIR fluorescence imaging and induction of genuine autophagy mediated chemotherapy. Nanoscale 10(22):10467–10478. https://doi.org/10.1039/C8NR02429D
291. Jayapaul J, Arns S, Lederle W, Lammers T, Comba P, Gätjens J, Kiessling F (2012) Riboflavin carrier protein-targeted fluorescent USPIO for the assessment of vascular metabolism in tumors. Biomaterials 33(34):8822–8829. https://doi.org/10.1016/j.biomaterials.2012.08.036
292. Chee HL, Gan CRR, Ng M, Low L, Fernig DG, Bhakoo KK, Paramelle D (2018) Biocompatible peptide-coated ultrasmall superparamagnetic iron oxide nanoparticles for in vivo contrast-enhanced magnetic resonance imaging. ACS Nano 12(7):6480–6491. https://doi.org/10.1021/acsnano.7b07572
293. Girard OM, Du J, Agemy L, Sugahara KN, Kotamraju VR, Ruoslahti E, Bydder GM, Mattrey RF (2011) Optimization of iron oxide nanoparticle detection using ultrashort echo time pulse sequences: comparison of T1, T2*, and synergistic T1–T2* contrast mechanisms. Magn Reson Med 65(6):1649–1660. https://doi.org/10.1002/mrm.22755
294. Luo Y, Kim EH, Flask CA, Clark HA (2018) Nanosensors for the chemical imaging of acetylcholine using magnetic resonance imaging. ACS Nano 12(6):5761–5773. https://doi.org/10.1021/acsnano.8b01640
295. Bar-Shir A, Avram L, Yariv-Shoushan S, Anaby D, Cohen S, Segev-Amzaleg N, Frenkel D, Sadan O, Offen D, Cohen Y (2014) Alginate-coated magnetic nanoparticles for noninvasive MRI of extracellular calcium. NMR Biomed 27(7):774–783. https://doi.org/10.1002/nbm.3117
296. Perez-Balderas F, van Kasteren SI, Aljabali AAA, Wals K, Serres S, Jefferson A, Sarmiento Soto M, Khrapitchev AA, Larkin JR, Bristow C, Lee SS, Bort G, De Simone F, Campbell SJ, Choudhury RP, Anthony DC, Sibson NR, Davis BG (2017) Covalent assembly of nanoparticles as a peptidase-degradable platform for molecular MRI. Nature Commun 8:14254. https://doi.org/10.1038/ncomms14254https://www.nature.com/articles/ncomms14254#supplementary-information
297. Henke PK, Pearce CG, Moaveni DM, Moore AJ, Lynch EM, Longo C, Varma M, Dewyer NA, Deatrick KB, Upchurch GR, Wakefield TW, Hogaboam C, Kunkel SL (2006) Targeted deletion of CCR2 impairs deep vein thombosis resolution in a mouse model. J Immunol 177(5):3388. https://doi.org/10.4049/jimmunol.177.5.3388
298. Yokoyama S, Ikeda H, Haramaki N, Yasukawa H, Murohara T, Imaizumi T (2005) Platelet P-selectin plays an important role in arterial thrombogenesis by forming large stable platelet-leukocyte aggregates. J Am Coll Cardiol 45(8):1280–1286. https://doi.org/10.1016/j.jacc.2004.12.071
299. Suzuki M, Bachelet-Violette L, Rouzet F, Beilvert A, Autret G, Maire M, Menager C, Louedec L, Choqueux C, Sabourat P, Haddad O, Chauvierre C, Chaubet F, Michel J-B, Serfaty J-M, Letourneur D (2014) Ultrasmall superparamagnetic iron oxide nanoparticles coated with fucoidan for molecular MRI of intraluminal thrombus. Nanomedicine 10(1):73–87. https://doi.org/10.2217/nnm.14.51
300. Xu J, Zhou J, Zhong Y, Zhang Y, Liu J, Chen Y, Deng L, Sheng D, Wang Z, Ran H, Guo D (2017) Phase transition nanoparticles as multimodality contrast agents for the detection of thrombi and for targeting thrombolysis: in vitro and in vivo experiments. ACS Appl Mater Interfaces 9(49):42525–42535. https://doi.org/10.1021/acsami.7b12689
301. Tang T, Valenzuela A, Petit F, Chow S, Leung K, Gorin F, Louie AY, Dhenain M (2018) In vivo MRI of functionalized iron oxide nanoparticles for brain inflammation. Contrast Media Mol Imaging 2018:3476476–3476476. https://doi.org/10.1155/2018/3476476

302. Gu L, Li X, Jiang J, Guo G, Wu H, Wu M, Zhu H (2018) Stem cell tracking using effective self-assembled peptide-modified superparamagnetic nanoparticles. Nanoscale 10(34):15967–15979. https://doi.org/10.1039/C7NR07618E
303. Naseroleslami M, Aboutaleb N, Parivar K (2018) The effects of superparamagnetic iron oxide nanoparticles-labeled mesenchymal stem cells in the presence of a magnetic field on attenuation of injury after heart failure. Drug Deliv Transl Res 8(5):1214–1225. https://doi.org/10.1007/s13346-018-0567-8
304. Sweeney SK, Manzar GS, Zavazava N, Assouline JG (2018) Tracking embryonic hematopoietic stem cells to the bone marrow: nanoparticle options to evaluate transplantation efficiency. Stem Cell Res Ther 9(1):204–204. https://doi.org/10.1186/s13287-018-0944-8
305. Garcés V, Rodríguez-Nogales A, González A, Gálvez N, Rodríguez-Cabezas ME, García-Martin ML, Gutiérrez L, Rondón D, Olivares M, Gálvez J, Dominguez-Vera JM (2018) Bacteria-carried iron oxide nanoparticles for treatment of anemia. Bioconjug Chem 29(5):1785–1791. https://doi.org/10.1021/acs.bioconjchem.8b00245
306. Khandhar AP, Wilson GJ, Kaul MG, Salamon J, Jung C, Krishnan KM (2018) Evaluating size-dependent relaxivity of PEGylated-USPIOs to develop gadolinium-free T1 contrast agents for vascular imaging. J Biomed Mater Res Part A 106(9):2440–2447. https://doi.org/10.1002/jbm.a.36438
307. Nimi N, Saraswathy A, Nazeer SS, Francis N, Shenoy SJ, Jayasree RS (2018) Multifunctional hybrid nanoconstruct of zerovalent iron and carbon dots for magnetic resonance angiography and optical imaging: an in vivo study. Biomaterials 171:46–56. https://doi.org/10.1016/j.biomaterials.2018.04.012
308. Xiao Y, Lin ZT, Chen Y, Wang H, Deng YL, Le Elizabeth D, Bin J, Li M, Liao Y, Liu Y, Jiang G, Bin J (2015) High molecular weight chitosan derivative polymeric micelles encapsulating superparamagnetic iron oxide for tumor-targeted magnetic resonance imaging. Int J Nanomed 10:1155–1172. https://doi.org/10.2147/IJN.S70022